Fisheries and Oceans Canada
Pêches et Océans Canada

Ecosystems and Oceans Science
Sciences des écosystèmes et des océans

Canadian Science Advisory Secretariat (CSAS)

Research Document 2021/049

Pacific Region

Spatial density models of cetaceans in the Canadian Pacific estimated from 2018 ship-based surveys

Brianna M. Wright, Linda M. Nichol, and Thomas Doniol-Valcroze

Pacific Biological Station
Fisheries and Oceans Canada
3190 Hammond Bay Road
Nanaimo, BC V9R 4C8

September 2021 (Erratum: March 2022)

Canada

Foreword

This series documents the scientific basis for the evaluation of aquatic resources and ecosystems in Canada. As such, it addresses the issues of the day in the time frames required and the documents it contains are not intended as definitive statements on the subjects addressed but rather as progress reports on ongoing investigations.

Published by:

Fisheries and Oceans Canada
Canadian Science Advisory Secretariat
200 Kent Street
Ottawa ON K1A 0E6

http://www.dfo-mpo.gc.ca/csas-sccs/
csas-sccs@dfo-mpo.gc.ca

ISSN 1919-5044
ISBN 978-0-660-40171-3 Cat. No. Fs70-5/2021-049E-PDF

Correct citation for this publication:

Wright, B.M., Nichol, L.M., Doniol-Valcroze, T. 2021. Spatial density models of cetaceans in the Canadian Pacific estimated from 2018 ship-based surveys. DFO Can. Sci. Advis. Sec. Res. Doc. 2021/049. viii + 46 p. (Erratum: March 2022)

Aussi disponible en français :

Wright, B.M., Nichol, L.M., Doniol-Valcroze, T. 2021. Modèles spatiaux de la densité des cétacés dans les eaux canadiennes du Pacifique fondés sur un relevé effectué par navire en 2018. Secr. can. de consult. sci. du MPO. Doc. de rech. 2021/049. viii + 49 p.

TABLE OF CONTENTS

LIST OF TABLES

LIST OF FIGURES

ABSTRACT

Many cetacean species were depleted in Canadian Pacific waters by commercial whaling, which ended in 1967. Although some populations have since shown evidence of recovery, there is limited information about the current abundance and geographic distribution of many species, particularly in difficult-to-survey offshore regions. This lack of baseline data hampers conservation status assessments, including estimating population-level impacts of anthropogenic activities. From July to early September 2018, we conducted ship-based surveys of cetaceans throughout the coastal and offshore waters of British Columbia. Density surface modelling (DSM) was used to produce spatially-explicit abundance estimates and distribution maps for four commonly-encountered cetacean species: the humpback whale (*Megaptera novaeangliae*), fin whale (*Balaenoptera physalus*), Dall's porpoise (*Phocoenoides dalli*) and harbour porpoise (*Phocoena phocoena*). We estimated abundances of 7,030 (95% CI = 5,733-8,620) humpback whales, 2,893 (95% CI = 2,171-3,855) fin whales, 23,692 (95% CI = 19,121-29,356) Dall's porpoises and 5,207 (95% CI = 2,769-9,793) harbour porpoises throughout Canadian Pacific waters. Our results complement design-based abundance estimates calculated from the same survey data, and can be compared with past habitat modelling studies and historical whaling catch data to estimate the extent of recovery of previously harvested populations. The return of these predators to habitats from which they were previously extirpated will have important ecosystem-level implications. The DSM results can contribute to calculations of Potential Biological Removal estimates to inform fisheries bycatch, as well as providing spatial data that can be used to assess the risk of entanglements, ship strikes, acoustic disturbance, and other anthropogenic threats.

INTRODUCTION

Effective conservation of animal species requires recent and accurate estimates of population abundance and distribution. In particular, knowledge of the spatial densities of cetaceans is necessary to estimate the population-level impacts of threats that overlap with parts of their ranges, such as entanglement in fishing gear, vessel strikes, ocean noise, and other anthropogenic stressors.

In British Columbia (BC), many populations of large cetaceans were severely depleted or extirpated by commercial whaling. Shore-based whaling ended in BC in 1967, however Japanese and Soviet factory ship whaling continued until 1975 in the northeast Pacific, including portions of offshore Canadian waters (Ford 2014). Since then, cetacean populations have shown signs of recovery, with potentially large ecosystem-level effects.

Data on abundance trends and range expansion are lacking for most marine mammal species. Obtaining these data for cetaceans is often difficult due to their large home ranges and ability to move quickly within their habitats, and to the logistical challenges associated with surveying offshore areas. To meet the new requirements of the U.S. Marine Mammal Protection Act, DFO Science completed the Pacific Region International Survey of Marine Megafauna (PRISMM), a large-scale survey of inshore and offshore waters in the summer of 2018. Its objectives were to provide updated abundance estimates and distribution data for large marine species in Pacific Canadian waters. In addition, the sightings and density data are essential inputs to the habitat modelling exercises used to support future Critical Habitat designations and Marine Protected Areas.

Here, we provide spatially-explicit estimates of current abundance for four cetacean species throughout the Canadian Pacific that complement the design-based abundance estimates obtained using the same systematic survey data (Doniol-Valcroze et al., in press). The spatially-explicit abundance estimates were produced using a two-stage approach that involved fitting detection functions to model the probability of observing animals away from the trackline, and then building density surface models (DSM) to estimate abundance from detectability-corrected count data (Miller et al. 2013). Although habitat variables were considered, this analysis was not meant to provide predictions of habitat suitability for these species or to elucidate the relationships between cetacean spatial distributions and the dynamic environmental parameters that drive them. Instead, this model-based approach was undertaken to produce maps of cetacean densities throughout Canadian Pacific waters, which can be used to inform management scenarios (i.e. estimating spatial overlap of cetaceans with human activities). In addition, DSM can often achieve improved precision in abundance estimates compared to a design-based approach because they are able to account for some of the between-transect variation present in the data (Miller et al. 2013).

METHODS

SHIP-BASED SURVEYS

A line transect survey for cetaceans, the Pacific Region International Survey of Marine Megafauna (PRISMM), was conducted throughout the coastal and offshore waters of British Columbia, Canada from two vessel platforms, the CCGS *John P. Tully* and the CCGS *Tanu*, between July and early September, 2018. The survey design is described in detail by Doniol-Valcroze et al. (in press). During the survey, two observers were stationed on the deck above the navigation bridge, each scanning continuously on either side of the transect line using 7x50 Fujinon binoculars. Information about sightings and any changes in environmental conditions were relayed via Ultra High Frequency radio to a data recorder on the navigation deck, who entered the information on a laptop computer equipped with Mysticetus software (Steckler & Donlan 2018). Radial distances to sightings were determined using the binocular's reticles (or estimating distance by eye if animals were close to the vessel), and radial angles were measured using electronic angle boards made from digital protractors. An additional observer used Fujinon 25x150 MTM pedestal-mounted binoculars to assist the two primary observers with species identifications and group size counts after initial sightings had been reported by the primary observers. The position and speed of the survey vessel were transmitted to the data recorder's laptop using a GPS once every 10 or 30 seconds. Vessels travelled at survey speeds of approximately 10 knots. PRISMM field protocols are described in greater detail by Doniol-Valcroze et al. (in press).

Perpendicular distances to sightings were calculated from the radial distance and angle measurements using established methods described by Buckland et al. (2001). Sightings for which perpendicular distances could not be calculated, or which had uncertain species identifications, were discounted from further analysis. Only four species were encountered with sufficient frequency during PRISMM to proceed with DSM analysis: the humpback whale (*Megaptera novaeangliae*), fin whale (*Balaenoptera physalus*), Dall's porpoise (*Phocoenoides dalli*), and harbour porpoise (*Phocoena phocoena*).

DETECTION FUNCTIONS

This analysis used the same detection functions (DFs) as Doniol-Valcroze et al. (in press), fit using the same methodology, which we briefly describe here. DFs were fit to perpendicular distance data associated with sightings of each of the four species using the "ds" function in the R package "Distance" (Miller, 2017). A detection function is necessary for accurately estimating animal densities from visual survey data because it quantifies the probability that an animal is detected, given its distance from the survey trackline (Buckland et al. 2001). Candidate DF models included half-normal, hazard-rate and uniform keys fit using either conventional distance sampling (CDS, with and without adjustment terms), or using multi-covariate distance sampling (MCDS) and combinations of the following detectability covariates: visibility, Beaufort sea state, observer, vessel, and group size. Beaufort sea state and visibility categories were pooled prior to DF fitting to ensure a sufficiently high number of sightings within each covariate level.

We first fit a key-only CDS detection function and then began adding covariates using a stepwise forward selection process, starting with single-covariate MCDS detection functions. Comparison of AIC (Akaike Information Criterion) values between the CDS (key-only) and MCDS candidate detection functions was used to determine whether a covariate should be retained. Additional covariates were added to the MCDS detection function as long as the resulting AIC value of the fitted model continued to improve. In addition to AIC values, we also used quantile-quantile plots to assess the relative fits of candidate DFs. Once a reasonable detection function had been chosen, we applied a right-truncation distance equivalent to the distance at which the probability of detection, $\hat{f}(x)$, dropped to approximately 0.15, as recommended by Buckland et al. (2001). By truncating the perpendicular distance data in this way, we were able to minimize the number of lower-value inclusion probabilities, thereby reducing the bias in the resulting Horvitz-Thompson-like estimators of abundance (D.L. Borchers, University of St. Andrews, St. Andrews, UK, pers. comm.).

DENSITY SURFACE MODELS

We used DSM to estimate abundance for each of the four cetacean species and predict patterns of animal density in each stratum based on various environmental covariates.

Study Area Stratification

Since the habitat characteristics that explain cetacean abundance and distribution in offshore versus coastal areas were likely to be different, the survey was stratified to separate offshore from inshore waters, the latter of which was further divided into two smaller strata, for a total of three different strata (one for the offshore, and two for coastal areas: the north coast and the Salish Sea; Figure 1). Note that the post-stratification scheme for dividing the inshore areas differs slightly from that used for the design-based abundance estimates by Doniol-Valcroze et al. (in press). A separate spatial model was built for each species and stratum, while the detection functions were species- but not stratum-specific. These strata did not extend beyond Canada's Exclusive Economic Zone (EEZ), a boundary which represented the extent of the ship survey effort. The offshore stratum included all effort and sightings made from the CCGS *John P. Tully*, with Canada's EEZ forming its boundaries to the north, south and west, and the eastern boundary along the west coasts of Haida Gwaii and Vancouver Island. Combined, the north coast and Salish Sea strata encompassed the effort and sightings made from the CCGS *Tanu*. The boundaries of the north coast stratum were similar to those of a previously delineated ecologically important area, the North Shelf Bioregion (DFO 2009). Its southern boundary was at the northern end of the Strait of Georgia, on the east side of Vancouver Island, while its northern edge ended at Canada's border with Alaska. South of this, the Salish Sea stratum included the Strait of Georgia and the Canadian (northern) half of Juan de Fuca Strait. A similar boundary between the Salish Sea and north coast strata was also used by Best et al. (2015) in an earlier DSM study of marine mammals in coastal BC. The respective areas of the three strata were 10,001 km^2 for the Salish Sea, 72,621 km^2 for the north coast, and 353,489 km^2 for the offshore.

Environmental Covariates

Within each stratum, continuous portions of the visual survey trackline were divided into approximately equal-sized segments, with a target length of 5 km, using methodology described in detail by Becker et al. (2010). The estimated per-segment abundance, which accounted for the probability of detection as a function of the sighting/object level DF covariates (see Miller et al. 2013 for more detail), was used as the response variable in the DSMs for all species except harbour porpoises. For harbour porpoises, the lack of covariates (other than distance) present in the best-fit DF allowed us to model the counts per segment as the response. Explanatory environmental covariates were measured at the midpoints of each of the segments. Explanatory covariates tested in models of all three strata included easting (X) and northing (Y) (typically modelled as a bivariate smoother), water depth, slope, terrain ruggedness index (TRI), and Euclidean distance to nearest shore. The covariates of distance to the 200 and 1,000 m bathymetric contours (i.e., the continental shelf edge and continental slope) were only included in models for the offshore stratum, while root mean square (RMS) of tidal current speed and distance to nearest area of high tidal current speed (m) were only relevant to the inshore strata (north coast and Salish Sea). Tidal current speed covariates were not included in any of the offshore models because tidal influence on currents diminishes with distance from the coast.

Water depths were extracted from a digital elevation model (DEM) raster with a resolution of 75 x 75 m. Both slope and TRI were calculated from the DEM using the "terrain" function in the R package "raster" (Hijmans 2019). TRI is the mean of the absolute differences between the depth value of a raster cell and the value of the eight surrounding cells. Slope and the related covariate of TRI were chosen as potentially significant predictors of cetacean abundance, as these parameters are both ways of identifying regions with increased bathymetric complexity. Cetaceans and other marine predators are often found in areas with steeper topographical relief or high benthic rugosity because these features are associated with higher primary productivity or prey aggregations (Bouchet et al. 2015, Croll et al. 1998, Yen et al. 2004).

Similarly, we also selected the 200 and 1,000 m contours as potentially important bathymetric features because they correspond to the continental shelf break and continental slope, a steep area in which the relatively shallow waters of the continental shelf give way to much deeper water over the abyssal plain. The edge of the shelf is often characterized by upwelling and tidal mixing that result in increased primary productivity and concentrations of planktonic prey (Croll et al. 1998, Springer et al. 1996) and, thus, has been found to be a significant predictor of baleen whale presence in previous studies (Dalla Rosa et al. 2012, Harvey et al. 2017, Nichol et al. 2017, Yen et al. 2004). Euclidean distances to the 200 or 1,000 m isobaths were calculated in one of three possible ways: directional (distances were negative if the segment midpoint was east of the bathymetric contour (i.e., on the continental shelf) and positive if west of the contour), absolute (distances were positive regardless of the relative direction of the segment midpoint to the contour), and zero-positive (on-shelf segment midpoints were given a value of zero, whereas those west of the contour were given positive distance values). Since the continental shelf break runs roughly north to south in the Canadian Pacific, it was also possible to combine distances to the 200 m or 1,000 m bathymetric contour (covariates that typically had east-west gradients) in a bivariate smoother with northing (Y) in some models.

RMS tidal current speed and areas of high tidal speed modelled by Foreman et al. (2000) were obtained as spatial layers from the British Columbia Marine Conservation Atlas. Distances to high tidal current areas were calculated as the Euclidian distances from segment midpoints to the edge of the closest spatial polygon representing a high current area. These two measures of tidal current speed were included as covariates for the inshore strata, since tidal currents can act to aggregate the zooplankton prey of baleen whales in coastal regions (Rogachev et al. 2008). Tidal currents have also been shown to predict relative distributions and densities of harbour porpoises (Embling et al. 2010, Johnston et al. 2005). All covariates were calculated in SI units (i.e., metres for distances/depths, m s^{-1} for tidal current speed, and northing/easting in metres for position data) and were standardized prior to model fitting. All maps are displayed using the Albers Equal Area Conic projection.

Model Fitting

We fit Generalized Additive Models (GAMs) in the “dsm” package in R (Miller et al. 2019) to produce spatially-explicit estimates of cetacean abundance. Prior to model construction, we conducted data exploration following protocols outlined by Zuur et al. (2010). We assessed collinearity between explanatory covariates by calculating Variance Inflation Factors (VIF) and sequentially removing variables until all covariates had VIF values below a pre-defined threshold of three (Zuur et al. 2010). Since the sighting location covariates (easting and northing) were modelled together as a bivariate smoother, we could not test them for collinearity with univariate model terms, and so the s(X,Y) term was always included in preliminary model runs.

For each species and stratum, we ran both location-only (spatial coordinate, or X,Y) models and global models that also included combinations of the other environmental covariates (as long as they were not collinear with one another). For instance, the six covariates (i.e., directional, absolute or zero-positive) representing distances to either the 200 m or 1,000 m isobath were never included in the same model because they were always collinear. Global models were initially run with all possible (i.e., non-collinear) covariates, all of which were treated as non-linear, penalized thin plate regression spline smoothers (basis type was set to “ts” in the mgcv package). This “shrinkage” approach (Marra and Wood 2011) allowed us to undertake model term selection in a single step without the problem of path dependence that can occur when using stepwise selection. This is because this smooth class also penalizes the null space slightly, and the whole term can therefore be shrunk to zero. A similar approach was used by the National Oceanic and Atmospheric Association (NOAA) in analysis of cetacean survey data from the California current ecosystem (Becker et al. 2020). In one case, a Duchon spline was fit instead of a shrinkage spline. Covariates with effective degrees of freedom (edf) <1 were deemed to have poor to no explanatory power and were dropped from the model unless $p \leq 0.01$, in which case they were retained in one of the candidate model options. Plots of the GAM smooth functions and their associated standard error bounds were also examined, as these also contain information that can support the decision to either drop or retain a covariate term. The relative magnitudes of each smoother’s basis size (k) and its resulting edf value were examined for the presence of unrealistically high values that could indicate over-fitting and to also ensure that smooth functions were given sufficient freedom to describe the underlying covariate relationship (k was then adjusted accordingly if needed). Smoothing parameter estimates were optimized using restricted maximum likelihood (REML), as recommended by Miller et al. (2013). REML has been found to out-perform generalized cross-validation (GCV) for estimation of smoothing parameters (Marra & Wood 2011). To address zero-inflation, which is a common cause of overdispersion in count data, we considered candidate models fit with negative binomial or Tweedie response distributions (log link) in addition to the quasi-Poisson distribution.

Model Selection and Validation

Selection among the resulting candidate models followed a two-step process. First, we selected the best-fit model from among the candidate GAMs with the same response distribution using AIC values. Then, we selected between the top models of differing response distributions by comparing quantile-quantile (QQ) plots of the model residuals generated using the qq.gam function (Augustin et al. 2012) in the R package ‘mgcv’. These QQ plots graphed the deviance residuals against reference bands that were produced by repeatedly simulating new response data from the fitted model 1,000 times. Departure of the residuals from the bounds of the reference bands indicate a mis-specification of the model (see Augustin et al. 2012) and thus can be used to assess fit and eliminate a model from the candidate set.

After a best-fit model was selected for each species-stratum combination, we undertook several validation tests to ensure its compliance with the underlying modelling assumptions and to check that its predictions were biologically reasonable. These tests included ensuring no patterns remained in the residuals (by using the “rqgam.check” function to generate randomized quantile residual plots), assessing spatio-temporal autocorrelation in the residuals (using the “dsm.cor” function, Miller et al. 2019), and visually comparing the model-predicted densities with actual survey observations. We also assessed overdispersion of residuals after the models were fit using the following formula:

$$\frac{\sum(e^2)}{N-P}$$

where e represents the Pearson residuals from the model, N is the sample size (i.e., number of segments), and P is the number of model parameters. Values greater than 1 indicated the presence of overdispersion, which can stem from a variety of causes including possible zero-inflation.

Density Predictions and Abundance Estimates

Once we had selected the best-fit GAM for each species and stratum, we used it to predict the density of individuals across a 5 x 5 km gridded surface of the stratum. This grid resolution was chosen because it was similar to the target segment length (5 km) and was also used successfully in past spatial modelling studies of cetaceans in this region (Nichol et al. 2017). The 5 km segment length was selected based upon previous studies (e.g., Becker et al. 2010), taking into consideration the distances at which observers might reasonably be able to detect animals, such that average segment length and effective strip width did not differ too greatly in magnitude. To generate this prediction, the significant explanatory covariates from the best-fit model were averaged across each cell of the 25 km^2 predictive grid, or in the case of spatial coordinate or distance covariates (e.g., easting, northing, distance to shore, distance to 200 or 1,000 m isobaths), values were measured from the grid cell's centroid. The total abundance of individuals across each stratum was determined by summing the predicted densities of all 5 x 5 km grid cells. Uncertainty in these abundance estimates was quantified by calculating 95% confidence intervals and coefficients of variation (CVs) using the delta method, in which the GAM uncertainty is combined with the detection function uncertainty for a total CV measure. This variance estimation method also produces CVs for each of the detection function and DSM components, and assumes that the GAM and DF are independent. Since the detection function is the same in all strata, we used equations 3.121 to 3.125 in Buckland et al. (2001) to separate the variance into two components, one of which is estimated independently in each stratum and the other (i.e., the detection function component) that is common across strata and should only be included once in the variance of the total abundance estimate.

RESULTS

VISUAL SURVEY EFFORT AND SIGHTINGS

The PRISMM survey was conducted between July 4 and September 5, 2018, and produced a total of 11,267.4 km of visually surveyed effort trackline and associated sightings that were used for the DSMs. This included both on-effort transects as well as transiting legs that occurred between some of the transects, but for which observers still logged sightings and effort as if they were on a regular transect. The effort used in the DSM analysis also included some transects that were repetitively surveyed (145 transects were surveyed once, while 25 transects were surveyed 2-4 times). Repeated transects were segmented and analyzed within the DSM as though they were independent. One of the advantages of DSM abundance estimation over design-based methods is that it does not rely on a random sampling design (Miller et al. 2013), and, therefore, repeated transects may be included. The total number of detected sightings, individuals, and the mean group size for each cetacean species are presented in Table 1. Maps of sightings by group size, as well as realized visual survey effort, are presented for each of the four modelled species in Figure 2. Mean segment length in the DSM analysis was 4,972 m (SD = 594 m), with 1,242 segments occurring in the offshore, 854 in the north coast, and 170 in the Salish Sea stratum, respectively.

DETECTION FUNCTIONS

The best-fit detection functions are described in greater detail by Doniol-Valcroze et al. (in press). The best-fit humpback whale detection function was a hazard-rate key with the covariates of vessel, observer, sea state, visibility and group size (Figure 3, top left). It had a right-truncation distance of 4,000 m and an effective strip (half)-width (ESW) of 1,479 m. The best-fit fin whale detection function was a hazard-rate key with covariates visibility and group size (Figure 3, top right). It had a right-truncation distance of 5,000 m and an ESW of 2,377 m.

The Dall's porpoise detection function was a half-normal key with visibility, sea state (Beaufort scale) and vessel as covariates, a right-truncation distance of 900 m and ESW of 499 m (Figure 3, bottom left). We used a half-normal key for Dall's porpoises (even though the hazard-rate key produced the best fit according to AIC) because half-normal detection functions help to reduce positive bias in estimated densities due to animals being attracted to the survey vessel (i.e., bow-riding) (Best et al. 2015, Turnock & Quinn 1991). Clustering of sightings very close to the vessel (Doniol-Valcroze et al., in press) indicated that at least some Dall's porpoises exhibited a positive movement response to the survey vessel's approach during PRISMM. Despite producing an improved AIC value, the observer covariate was excluded from the final DF for Dall's porpoises, as including it resulted in an extremely large CV which led to unreasonably high uncertainty in estimated abundances from the DSMs. This high uncertainty was likely due to the large number of factor levels (N = 22) in the observer covariate and thus the limited number of observations within each level. A CDS hazard-rate model with no covariates and a cosine(2,3) adjustment was selected as the best detection function for harbour porpoises. It had a right-truncation distance of 1,200 m and an ESW of 446 m (Figure 3, bottom right).

DENSITY SURFACE MODELS

Comprehensive tables providing lists of all candidate DSMs, their associated diagnostic parameters and abundance estimates are presented in Appendix A for each species and stratum. Appendix B provides maps of local place names for the BC coast that are mentioned in the Results and Discussion of this report.

Humpback Whale

Humpback whales were sighted more frequently (N = 767) than any other species of cetacean during PRISMM, for a total of 1,145 individual whales (Table 1). Of these sightings, those both within the right-truncation distance and for which perpendicular distances could be calculated totaled 671, which were then used for the DSM analyses. The majority of humpback whale sightings occurred in the offshore stratum (N = 370), while the north coast and Salish Sea strata had 263 and 38 sightings, respectively. Mean group size for humpback whales was 1.5 (SD = 1.3) animals (Table 1).

The offshore stratum had a best-fit DSM for humpback whales with a single explanatory covariate, which was a bivariate smooth of distance from the 1,000 m bathymetric contour (calculated as a +/- directional term) and northing (i.e., Y coordinates) (edf = 17.5, Table 2). This GAM had a Tweedie error distribution. The total estimated abundance of humpback whales in the offshore stratum was 4,935 (95% CI = 3,865-6,303; total CV = 0.13, Table 2). The model predicted the highest densities of humpback whales in this region (>2 whales per 25 km^2 grid cell) along the eastern side of the continental shelf break, between the latitudes of Moresby Island (Haida Gwaii) and Clayoquot Sound (Vancouver Island) (Figure 4). Very few humpback whales were predicted to be found in deeper waters off the western side of the shelf break.

In the north coast stratum, the best-fit DSM was a GAM with a Tweedie response distribution and the environmental covariate of sighting locations (easting and northing, modelled as a bivariate smoother, edf = 24.0, Figure 5). This model estimated a total abundance of 1,816 humpback whales (95% CI = 1,403-2,351; total CV = 0.13) throughout the north coast stratum (Table 2). The highest densities of humpbacks in the north coast (≥2 individuals per 25 km^2) were predicted in the submarine canyons off of southern Haida Gwaii (see Figure B1 in Appendices for location), on the BC mainland regions of Caamaño Sound, Fitz Hugh Sound and River's Inlet. Moderate humpback densities (at least 1 individual per 25 km^2 cell) were also predicted in western Dixon Entrance, Chatham Sound, Hecate Strait, and Queen Charlotte Sound/Strait off northeastern Vancouver Island (Figure 5).

In the Salish Sea, the best-fit DSM for humpback whales was a negative binomial GAM with only a single explanatory covariate, a bivariate smooth of sighting location (edf = 1.9, Figure 6). It predicted a total of 279 animals (95% CI = 130-596; total CV 0.40) for this stratum (Table 2). Juan de Fuca Strait contained the highest predicted densities of humpback whales (>3 individuals per 25 km^2 cell) in the stratum, while the northern Strait of Georgia was also predicted to have moderate numbers of humpback whales (1-2 individuals per 25 km^2, Figure 6). The combined abundance estimate for humpback whales across all three strata was 7,030 (95% CI = 5,733-8,620; total CV = 0.10, Table 2).

Fin Whale

A total of 235 sightings of fin whales were made during PRISMM, comprising a total of 357 individuals (Table 1). Within the right-truncation distance of the detection function, perpendicular distances were calculated for 213 of these sightings, which were then used for the DSM analyses. The majority of fin whale sightings occurred in the offshore stratum (N = 184), while only 29 sightings were made in the north coast stratum. No spatial model or associated abundance estimate was produced for fin whales in the Salish Sea, because this species was not detected within this stratum during PRISMM. Mean group size for fin whales was 1.5 (SD = 0.9) animals (Table 1).

The best-fit DSM for fin whales in the offshore stratum was a Tweedie GAM with the explanatory covariates of sighting location (easting and northing, modelled together as a bivariate smooth, edf = 17.0) and distance from the 1,000 m bathymetric contour (calculated as absolute values and modelled as a non-linear smoother, edf = 5.0) (Figures 7 and 8). It produced an estimated abundance of 2,732 fin whales (95% CI = 2,044-3,651; total CV = 0.15, Table 2). The highest densities of fin whales in the offshore stratum were predicted to occur immediately west of the continental shelf break (1,000 m bathymetric contour), primarily at latitudes between Moresby Island (southern Haida Gwaii) and Barkley Sound on southern Vancouver Island (Figure 7). The main hot-spot of fin whale density in this region occurred west of the shelf break at approximately the same latitude as Brooks Peninsula off western Vancouver Island. The highest densities of fin whales were predicted to be closest to the shelf break feature, with densities dropping steadily until ~200 km west of the shelf break, when they began to level off somewhat (Figure 8). Very few fin whales were predicted to occur in continental shelf waters east of the shelf break (Figure 7).

For the north coast stratum, the best fit DSM for fin whales was a negative binomial GAM with a bivariate smooth of sighting location (i.e., easting and northing) as the only explanatory covariate (edf = 10.7, Figure 9). This model estimated a total abundance of 161 fin whales (95% CI = 64-407; total CV = 0.50, Table 2) throughout the north coast. The highest predicted densities occurred in central Hecate Strait, the submarine canyon features southeast of Haida Gwaii, and the western side of Dixon Entrance (Figure 9). Together, the north coast and offshore DSMs predicted a total abundance of 2,893 fin whales (95% CI = 2,171-3,855; total CV = 0.15) for the Canadian Pacific (Table 2).

Dall’s Porpoise

A total of 287 sightings of 845 individual Dall’s porpoises were made during the PRISMM survey (Table 1). They were the most frequently sighted odontocete. Within the right-truncation distance of the detection function, perpendicular distances could be calculated for 239 of these sightings, which were then used for the DSM analyses. Most Dall’s porpoise sightings occurred in the offshore (N = 100) and north coast (N = 112) strata, with only 27 sightings in the Salish Sea. Dall’s porpoises had an average group size of 2.9 (SD = 1.8, Table 1).

The best-fit DSM for Dall's porpoises in the offshore had a Tweedie error distribution and a bivariate smooth of distance from nearest shore and northing (edf = 2.1, Figure 10) as its only explanatory covariate. Dall's porpoises occurred at moderate densities (~1-4 individuals per 25 km^2 cell) throughout the majority of the offshore stratum, except for the southwestern portion (Figure 10), and had a total estimated abundance of 17,934 (95% CI = 13,818-23,275; total CV = 0.13, Table 2).

In the north coast stratum, the selected DSM for Dall's porpoises had a Tweedie distribution and a bivariate smooth of sighting location (edf = 15.9, Figure 11) as its only covariate. Total estimated abundance in this stratum was 5,178 Dall's porpoises (95% CI = 3,756-7,138; total CV = 0.16, Table 2). The highest predicted densities of Dall's porpoises (≥4 individuals per 25 km^2) occurred in northern Hecate Strait, Chatham Sound and Portland Inlet, as well as throughout Laredo Sound and Milbanke Sound on the central coast of BC (Figure 11). However, moderate densities (2-4 individuals per 25 km^2) of Dall's porpoises were also found throughout Dixon Entrance, mid-Hecate Strait, and off of northeastern Vancouver Island in the Queen Charlotte and Johnstone Straits (Figure 11).

The Salish Sea best-fit DSM for Dall's porpoises was a Tweedie-distributed GAM with the single explanatory smoother of distance to nearest shore (edf = 1.6, Figures 12 & 13), fit using a Duchon spline. The total number of Dall's porpoises predicted in this region was 580 (95% CI = 313-1,075; total CV = 0.32, Table 2). The relationship between Dall's porpoise density and distance from shore was positive, with more porpoises predicted to occur in the central Strait of Georgia than near the shorelines of Vancouver Island or mainland BC (Figure 12), although the relationship leveled off at the greatest distances from shore (>10 km, Figure 13). The confidence intervals at these greater distances were very wide, which is not surprising given the low number of segments sampled at these distances (see x-axis rug plot, Figure 13). Therefore, the relationship between predicted Dall's porpoise densities and distance from shore becomes much more uncertain as distance from shore increases. The overall estimated abundance of Dall's porpoises in all three strata combined was 23,692 (95% CI = 19,121-29,356; total CV = 0.11, Table 2).

Harbour Porpoise

Harbour porpoises were sighted 246 times during PRISMM, representing a total of 403 individuals (Table 1). Within the detection function's right-truncation distance, perpendicular distances were calculated for 226 of these sightings. Most harbour porpoises were seen in the Salish Sea stratum (N = 161 sightings), whereas 54 sightings were made on the north coast. No spatial models were run for harbour porpoises in the offshore because only 11 sightings of this species were available for modeling in this stratum. The mean group size for harbour porpoises was 1.6 (SD = 0.9) animals (Table 1).

The best-fit DSM for harbour porpoises in the north coast stratum was a negative binomial GAM with a single explanatory covariate, a bivariate smooth of sighting locations (easting and northing, edf = 8.7, Figure 14). A total abundance of 1,314 harbour porpoises (95% CI = 648-2,664; total CV = 0.37, Table 2) was estimated for the north coast. The highest densities of harbour porpoises in this stratum (>2 individuals per 25 km^2 grid cell, see Figure 14) occurred over Dogfish Bank (east of Graham Island, Haida Gwaii), in Chatham Sound and Portland Inlet (Figure 14, Inset A), and in the inlets east of Vancouver Island (Knight and Bute Inlets, Figure 14, Inset B).

In the Salish Sea stratum, the top-ranked harbour porpoise DSM was also a negative binomial GAM with the single explanatory covariate of sighting locations, modelled as a bivariate smoother (edf = 20.1, Figure 15). Predicted harbour porpoise abundance in the Salish Sea was

3,893 animals (95% CI = 1,991-7,611; total CV = 0.35, Table 2). The model predicted the highest densities of harbour porpoises (>30 individuals per 25 km^2 grid cell) east of the Saanich Peninsula and southeast of Victoria and Esquimalt in Juan de Fuca Strait (Figure 15). Moderately high densities (20-40 individuals per 25 km^2) were also predicted in Boundary Bay, south of Vancouver, as well as in the central and northern portions of the Strait of Georgia (Figure 15). The total estimated abundance of harbour porpoises in the Canadian Pacific (north coast and Salish Sea strata combined) was 5,207 (95% CI = 2,769-9,793; total CV = 0.33, Table 2).

DISCUSSION

In combination with Doniol-Valcroze et al. (in press), this analysis represents the most current and spatially comprehensive effort to estimate the abundance and distribution of cetaceans in Canadian Pacific waters.

MODEL LIMITATIONS AND SOURCES OF UNCERTAINTY

Although PRISMM provided excellent spatial coverage of the study area, it was limited temporally because the data were collected during a single season (summer) and single year (2018). As such, we are unable to predict interannual or seasonal fluctuations in abundance and density of cetaceans in Canadian Pacific waters. This may be particularly important in the case of migratory species, such as the humpback whale, which is much less prevalent in the northeast Pacific during its breeding and calving season (winter). Having repeated surveys within a year or multiple years of survey data available would allow models to account for more of the natural, within- and between-year and variation in animal abundance and distribution that is not captured in data from a single survey. It is likely that the accuracies of both the abundance estimates and the model-predicted spatial densities would improve with the inclusion of more surveys.

Dynamic spatiotemporal environmental covariates, which are usually extracted from satellite data or ocean models (e.g. sea surface temperature, chlorophyll-*a* concentration, etc.), are often included in habitat models for cetaceans (e.g. Dalla Rosa et al. 2012, Harvey et al. 2017) but were not considered in these DSMs. The goal of this study was not to produce habitat models explaining the underlying biological drivers of cetacean spatial distributions, but to estimate overall abundance with an improved degree of precision by including a spatially-explicit component to explain between-segment variation in the number of sightings. It is unlikely that inclusion of time-varying, satellite-derived environmental variables would appreciably change the abundance estimates we present here. In addition, time-varying, satellite-derived environmental variables are often computed over multiple time periods (e.g. monthly composites) so that shifts in animal distribution or abundance linked to either season or survey year may be explained. Given the single season, single year nature of the PRISMM dataset, an analysis of seasonal or inter-annual changes could not be considered. In the future, with more survey data available, we may build models that include these variables to improve upon our understanding of the underlying drivers of cetacean spatial distributions in the Canadian Pacific. However, satellite data availability in the northeast Pacific is also limited by factors such as cloud cover (Fox et al. 2017), which will likely restrict the use of such covariates to averages covering monthly (or possibly longer) time intervals.

As in the design-based abundance estimates from PRISMM (Doniol-Valcroze et al., in press), perception bias (Buckland et al. 2001) could not be estimated from the survey data that were collected. Therefore, abundance estimates from the DSMs will underestimate true population sizes because we cannot account for animals that were present on the surface to be detected, but were missed by observers near the trackline. In addition, the DSM analysis did not consider availability bias (animals missed because they were underwater and unavailable for detection by observers, Buckland et al. 2001). Correction factors for availability bias are proposed in Doniol-Valcroze et al. (in press) for the four species considered here, and could be applied directly to the DSM abundance estimates. It should be noted, however, that these correction factors rely on a small sample size of published studies, and that actual dive times of cetaceans are known to vary considerably depending on behavioural context (e.g., foraging, travelling, resting), dive depth and the time of day. Therefore, it is likely that using a single correction factor for the different strata would not properly account for the uncertainty around availability bias. Availability bias is also likely to have a much smaller relative impact on survey data collected from slow-moving ship platforms (like those used during PRISMM), compared to distance sampling conducted from fast platforms such as aircraft.

Spatio-temporal autocorrelation was present in most of the DSMs (7 of the 10 top-ranked models), however most models contained autocorrelation at lags of only a single survey segment. The Dall's porpoise DSM for the offshore stratum was the only model with greater autocorrelation, which was detected at lags of 1-3 segments. Including smooths of sighting locations (X,Y) in the models is one way of modelling spatial dependence in the residuals. Autocorrelation between segments can also be dealt with by fitting a mixed model (GAMM) with the same covariates as the original GAM, plus the addition of a moving-average correlation structure of order (p,0), where p equals the time lag (i.e., number of segments, nested within transects) over which the residuals were correlated. However, fitting GAMMs in "dsm" is complicated, requiring additional assumptions and often resulting in limited success (D.L. Miller, University of St. Andrews, St. Andrews, UK, pers. comm.), and there is also no way to compare candidate GAMMs using AIC values, as this metric is not generated for GAMMs. While we did attempt to fit GAMMs, we found that the spatial distribution of estimated densities from these models were often nonsensical and biologically unrealistic, and so this approach was abandoned in favour of retaining the more reliable and comparable GAMs. By not accounting for spatial autocorrelation, it is possible for p-values in the GAMs to misrepresent the order of importance and degree of significance of the coefficients for the different covariates (Dormann 2007).

ABUNDANCE AND PREDICTED DISTRIBUTIONS

Humpback Whale

An earlier density surface model by Best et al. (2015) estimated a total abundance of 1,092 (95% CI = 993-1,200) humpback whales in coastal BC from survey data collected between 2004-2008. While the Best et al. (2015) model covered an area roughly equivalent to the north coast and Salish Sea PRISMM strata combined, this earlier study did not detect any humpback whales in the Salish Sea region. Conversely, PRISMM had 38 sightings of this species in the Salish Sea, and our density model predicted an abundance of 279 individuals (95% CI = 130-596), which indicates that humpback whales have recolonized an area from which they were largely absent 10-14 years prior. Citizen science sightings submitted to the BC Cetacean Sightings Network (BCCSN) since 2009, while not effort-corrected, provide further evidence of a return of humpback whales to the Salish Sea (BCCSN, unpublished data). Compared to the Best et al. (2015) estimate of 1,092 humpback whales, our abundance estimate of 1,816 (95% CI = 1,403-2,351) humpbacks in the north coast stratum suggests a moderate increase due to either population growth or immigration of new individuals into this area. The regions of highest density in the Best et al. (2015) model are in agreement with the north coast regions highlighted by PRISMM, namely Dixon Entrance, Hecate Strait, the submarine canyons southeast of Haida Gwaii, and the larger inlets and sounds of the northern and central mainland coast of BC. The

Caamaño Sound and Kitimat fjord system which was highlighted by both the Best et al. (2015) and the PRISMM north coast model was also identified by Keen et al. (2017) as an important area in which humpback whales aggregate to feed during the summer months.

The Best et al. (2015) humpback whale DSMs included the static explanatory terms of latitude, longitude, depth, distance to shore, and slope, while our coastal DSMs (north coast & Salish Sea) were solely based on bivariate smooths of sighting locations. Despite being relatively simpler, our DSMs had slightly better explanatory power (deviance explained = 18-29% vs. 11-19%), but also much higher uncertainty (total CVs were 0.13 and 0.40, for the north coast and Salish Sea, respectively, versus 0.05 for the Best et al. model).

Dalla Rosa et al. (2012) used GAMs to predict humpback whale distribution from data collected during multiple non-systematic surveys of BC coastal waters between 2004-2006; however, this study did not provide an associated abundance estimate. The area modelled by Dalla Rosa et al. (2012) was roughly comparable to our north coast stratum, but also included the continental shelf waters off the west coast of Vancouver Island (part of our offshore stratum). Dalla Rosa et al. (2012) found humpback whale abundance to be linked to both static (latitude, depth, slope, distance to 100 m isobath) and time-varying (chlorophyll *a* concentration, net primary productivity, sea surface temperature (SST), distance to SST fronts, and surface salinity and temperature) environmental covariates. Areas of humpback whale concentration identified by Dalla Rosa et al. (2012) were in general agreement with important areas identified by the PRISMM DSMs, and included Dixon Entrance, Hecate Strait and the continental shelf waters of western Vancouver Island.

One area of humpback whale concentration identified by Dalla Rosa et al. (2012) that our model did not highlight was the continental shelf area off of southwest Vancouver Island and the entrance to Juan de Fuca Strait (La Perouse and Swiftsure Banks). This is likely because very few humpback whales were seen in this area during PRISMM (Figure 2), either because of poor detection conditions at the time of the survey, or because the ship passed through on a day when few individuals happened to be present. However, we know this area to be of importance to this species, as it was previously recommended for designation as Critical Habitat based on high and persistent seasonal aggregations of animals (Fisheries and Oceans Canada 2013). This area (as well as the entire continental shelf edge west of Vancouver Island) was also identified by Nichol et al. (2017) as an area of high encounter probability for humpback whales based on spatial models of effort-corrected aerial survey data.

Ford et al. (2009) produced a 2006 population abundance estimate of 2,145 (95% CI = 1,970-2,331) humpback whales in the coastal waters of BC using mark-recapture techniques applied to photo-identification data. While it covers a similar spatial area, this result is difficult to compare to the 2018 PRISMM north coast estimate (1,816 humpback whales), due to the inherent differences in the methodology and assumptions of a mark-recapture versus a distance-sampling approach. In addition, the Ford et al. (2009) estimate included the continental shelf waters off Vancouver Island, which were part of a different abundance estimate (offshore stratum) in the PRISMM study. A wider-ranging photo-identification study of humpback whales in 2004-2005 (SPLASH) predicted a total abundance of 19,056 animals in summer feeding areas throughout the North Pacific, including waters of the western continental United States and Canada, Alaska, the Aleutian Island chain, and the Russian Far East (Calambokidis et al. 2008). The current North Pacific-wide abundance of humpback whales is unknown, but our estimate of 7,030 individuals throughout the PRISMM survey area shows that a large proportion of the North Pacific humpback population uses Canadian Pacific waters in the summer.

The candidate DSMs for humpback whales in the offshore displayed instability in estimated abundances, which fluctuated from ~4,500 to 48,000 individuals depending on which combination of environmental covariates we included (see Appendix A). We have chosen a relatively conservative model (4,935 whales) based on its low AIC value and assessment of its QQ plot (Table 2), as well as a visual assessment of density predictions from the model (Figure 4), which display reasonable overlap with the actual sighting locations and are biologically reasonable for the species based on results from prior studies (e.g., Best et al. 2015, Dalla Rosa et al. 2012, Nichol et al. 2017). Other models (one of which had actually had a lower AIC value than the selected Tweedie model) produced abundance estimates and associated density predictions with unrealistically large numbers of whales (>100) in numerous 25 km^2 grid cells, and, thus, were discarded. For the north coast humpback whale DSM, the location-only model produced an AIC value that did not differ significantly (deltaAIC < 2, Appendix A) from the more complex model that also included smoothers for the two tidal speed covariates. Given that the shapes and uncertainty around these two additional tidal smoothers also indicated that they provided little additional explanatory power, we retained the simpler location-only DSM as the best-fit model. When covariates other than a bivariate location smoother were introduced into the Salish Sea humpback whale DSM, impossibly high abundance estimates resulted, as well as unrealistic spatial density distributions. This may have been due to insufficient variation in the distance from shore covariate values, which were quite low throughout the enclosed Salish Sea. For this reason, the location-only negative binomial model was retained despite its higher AIC value.

Overall, our DSM abundance estimate of 7,030 humpback whales for all three strata combined was just over half of that estimated using the design-based approach (12,116 whales, Doniol-Valcroze et al., in press). The lower DSM abundance can mainly be attributed to our very conservative offshore abundance estimate of 4,935 humpback whales, compared to the design-based estimate for the same stratum of 8,467 individuals. This difference, as well as the instability we experienced during fitting of the offshore DSMs, leads us to have greater confidence in the accuracy of the design-based estimate for the offshore region (despite the increased precision achieved by the DSM: total CV for offshore stratum = 0.13 versus 0.27 for the design-based offshore estimate).

Fin Whale

Best et al. (2015) estimated a total of 329 fin whales (95% CI= 274-395) from 2004-2008 surveys covering an area roughly equivalent to the 2018 PRISMM north coast stratum. Fin whale abundance in the Best et al. model was related to sighting locations, depth, distance to nearest shore and slope. Similarly, another effort-corrected GAM produced from non-systematic ship survey data (2002-2014) collected in almost the same geographical region found that fin whale distribution was predicted by latitude, slope, and depth (Nichol et al. 2018). In comparison, our north coast PRISMM model was based solely on a bivariate smooth of sighting locations and produced a lower abundance estimate of 161 fin whales (95% CI = 64-407). Our abundance estimate for the north coast contains much higher uncertainty (total CV = 0.50) than Best et al.'s (CV = 0.09). While all three spatial models (Best et al. 2015, Nichol et al. 2018 and PRISMM) highlighted similar areas of high fin whale densities (e.g. central Hecate Strait, the submarine canyons southeast of Haida Gwaii, and Dixon Entrance), both the Best et al. (2015) and Nichol et al. (2018) models were based on a larger number of sightings (93 and 266, respectively) collected over multiple survey years, whereas our model was limited to only 29 sightings made during a single survey (Figure 2). It is possible that the relatively low number of sightings in the PRISMM model precluded it from finding significant relationships between fin whale abundance and additional environmental parameters, which would then have prevented the model from properly extrapolating abundance to unsurveyed areas. A photo-identification mark-recapture analysis of 2009-2014 data (Nichol et al. 2018) produced an abundance estimate of 405 fin whales (95% CI = 363-469) in an area encompassing most of the PRISMM north coast stratum (it included Hecate Strait, Queen Charlotte Sound and Caamaño Sound but not Dixon Entrance). While mark-recapture abundance estimates are not directly comparable those derived by distance sampling methods, the Nichol et al. (2018) estimate is similar to that of Best et al. (2015), in contrast to the lower 2018 PRISMM number.

Furthermore, PRISMM observers detected very few fin whales in both Caamaño Sound and the nearby Kitimat fjord system (Figure 9), either due to poor detection conditions or by chance. While Caamaño Sound was not identified by Best et al. (2015) as being particularly important, it was identified by Nichol et al. (2018), and has become known in years since the Best et al. (2015) surveys as a fin whale hot-spot. Multiple data sources (line-transect surveys, GPS tag data and passive acoustic recordings) have indicated that fin whales aggregate and feed in this area during the summer months (Keen 2017, Nichol et al. 2018), and whaling records indicate that this area was also used by fin whales historically (Nichol and Ford 2012).

Prior to PRISMM, there were no available estimates of abundance for fin whales in the offshore region of British Columbia. Aerial surveys conducted in 2012-2015, however, found that fin whales off of the west coast of Vancouver Island were more likely to be encountered in deeper water to the west of the continental shelf break. Fin whale distribution predicted by the PRISMM offshore DSM indicates a similar pattern, with more individuals located immediately west of the shelf break(Table 2, Figure 7 & 8).

No fin whales were encountered in the Salish Sea stratum during PRISMM, a result which is consistent with the earlier findings of Best et al. (2015). However, infrequent sightings of single fin whales in Juan de Fuca Strait and the Salish Sea have been recorded between 2005 and 2017 (Towers et al. 2018).

The design-based abundance estimate for fin whales in the Canadian Pacific (3,737, Doniol-Valcroze, in press) was slightly higher but comparable to the DSM estimate of 2,893 individuals, although the DSM estimate had greater precision (total CV = 0.15 versus 0.30 for design-based). The 95% CI for the DSM fin whale abundance estimate (2,171-3,855) was completely contained within the 95% CI of the design-based estimate (2,057-6,789).

Dall's Porpoise

Best et al. (2015) estimated an abundance of 5,303 (95% CI = 4,638-6,064) Dall's porpoises in an area roughly equivalent to the combined north coast and Salish Sea PRISMM strata. Our DSM analysis produced a very similar estimate of 5,758 for these two coastal strata combined, implying limited population growth or immigration from other areas during the 10 years that has elapsed between the two studies. Areas of high Dall's porpoise densities identified by both Best et al. (2015) and PRISMM in the north coast region included Dixon Entrance, northern and central Hecate Strait, Chatham Sound, the inlets of the central BC mainland coast, and the inshore waters of northeast Vancouver Island (Figure 11). Best et al. (2015) found Dall's porpoise abundance to be related to sighting locations, depth, distance to shore, slope, season and an inlet covariate, whereas our DSM for the north coast stratum relied solely on the northings and eastings of sighting locations.

In the Salish Sea stratum, Dall's porpoise abundance was related only to distance from nearest shore, meaning that this species was predicted to occur in greatest densities in the mid-channel areas of the Strait of Georgia and Juan de Fuca Strait (Figure 12). Both of these areas were also identified by Best et al. (2015) as having higher Dall's porpoise densities. Diet studies corroborate this finding, as Dall's porpoises in the Salish Sea feed on taxa that are typically found in deeper water (and deep water is usually located farther from shore), including walleye pollock, Pacific hake, and lanternfishes (Nichol et al. 2013). Hall (2011) also found that Dall's porpoises in the Salish Sea were found in areas with deeper water (151-200 m). Surveys of a ferry route crossing the southern Strait of Georgia in 2000-2001 (Keple 2002) also found that more Dall's porpoises were detected in the centre of the Strait as compared to closer to shore. Keple's (2002) summer abundance estimate was only 200 individuals (95% CI = 107-372) compared to our estimate of 580 Dall's porpoises (95% CI = 313-1,075), but Keple's study covered a smaller survey area of 2114 km^2 within our Salish Sea stratum, which was much larger at 10,001 km^2. Moran et al. (2018) similarly found that summer habitat use by Dall's porpoises in Prince William Sound, Alaska corresponded to areas with deeper water on average (242 m) that were also farther from shore (4,450 m). Depth itself was not significant in any of our Salish Sea models, likely because this stratum contained inlet segments that were located in deep water but were very close to shore and had no Dall's porpoise detections (Figure 12).

For the Salish Sea stratum, we selected a Tweedie model that fit the distance from shore smoother using a Duchon spline rather than the penalized thin plate regression spline used in the other candidate models. While the Duchon spline did not improve overall fit (according to AIC) compared to the same model using a thin plate regression spline, or its null equivalent (see Table A8), it did produce a more biologically realistic levelling out of predicted porpoise densities for the segments that were farthest from shore (Figure 13). However, as there were comparatively few segments sampled at these distances, the associated uncertainty around this smoother was relatively high. None of the negative binomial models we tested for either the Salish Sea or north coast stratum were found to contain any significant covariates, and so they were dropped from their respective candidate model sets.

No previous estimates of Dall's porpoise abundance exist for the offshore waters of BC. Our offshore DSM estimated a total 17,934 Dall's porpoises (95% CI = 13,818-23,275), spread relatively evenly across almost every part of this stratum except the southwest portion, which had very low densities (likely because hardly any Dall's porpoises were detected in this area during the survey, Figure 10). The Canadian Pacific-wide abundance estimates for Dall's porpoises from the design-based approach (29,377, Doniol-Valcroze et al., in press) was higher than the estimate from the DSM (23,692), however the 95% CIs overlapped considerably (21,541-40,065 for design-based, versus 19,121-29,356 for DSM). The DSM approach improved the overall precision somewhat (CV = 0.11) over the design-based method (CV = 0.16).

Harbour Porpoise

Best et al. (2015) estimated a total of 8,091 harbour porpoises (95% CI 4,885-13,401, CV = 0.26) in coastal BC waters (2004-2008 surveys), a region roughly equivalent to the combined north coast and Salish Sea PRISMM strata. Our estimated abundance for harbour porpoises in 2018 in this region was comparatively lower at 5,207 individuals total (1,314 for the north coast and 3,893 for the Salish Sea; Table 2). However, high densities of harbour porpoises were predicted in the following areas by both Best et al. (2015) and PRISMM: Dogfish Bank and northern Hecate Strait (east of Haida Gwaii), Chatham Sound, and Bute and Knight Inlets in the north coast stratum (Figure 14), and the northern/central Strait of Georgia, Boundary Bay and the waters off Victoria in Juan de Fuca and Haro Straits in the Salish Sea stratum (Figure 15). Hall (2011) identified a harbour porpoise hotspot in eastern Juan de Fuca Strait from sightings per unit effort (SPUE) data (collected between 1991-2008) that also corresponded well to the area of highest densities (>40 individuals/25 km^2) predicted by the PRISMM model (Figure 14), indicating that this region has been an important and persistent harbour porpoise habitat in the Salish Sea for many years. Keple (2002) found more harbour porpoises in the centre of the Strait of Georgia during surveys along a ferry route in 2000-2001, which matches our Salish Sea DSM predictions, however she did not detect any harbour porpoises north of Gabriola Island, whereas we had numerous sightings north of this location. Our north coast model identified

Dixon Entrance and Portland Inlet as potentially important areas of harbour porpoise aggregations on the north coast that were not highlighted in previous studies. Other studies provide harbour porpoise abundance estimates for smaller portions of the wider Salish Sea habitat, which are difficult to compare to the PRISMM estimate of 3,893 harbour porpoises in the entire Salish Sea stratum. For instance, Hall (2004) estimated 860 harbour porpoises (95% CI = 564-1,241) in a systematic distance-sampling analysis of Haro Strait and eastern Juan de Fuca Strait during the summers (April-October) of 2001 and 2002. A more recent study by Jefferson et al. (2016) estimated an abundance of 1,825 harbour porpoises (95% CI = 1,154-2,890, CV = 0.42) in the Canadian Gulf Islands from aerial survey data collected in 2015.

The Best et al. (2015) model found that harbour porpoise abundance was related to sighting locations, depth, distance to shore, slope and an inlet variable, whereas our best-fit model used only sighting locations (easting and northing). The lack of complexity of our DSM (in addition to our survey data being limited to a single season) may help to explain why our overall abundance estimate was lower. A model with more environmental covariates is better able to in-fill areas of potentially high density based on habitat characteristics shared with the locations of actual sightings. Without this additional information, a location-only (X,Y) model will assume little to no porpoise density in regions that were unsurveyed or that were surveyed but in which no porpoises were sighted (this is particularly problematic for areas surveyed during poor sighting conditions).

Although the north coast negative binomial model that also included a smooth of water depth produced a marginally better fit (according to AIC; see Appendix Table A9) than the model that only contained the sighting locations as an explanatory covariate, we selected the location-only model for this stratum. Depth was dropped because the density surface generated by the model that included it as a covariate resulted in unrealistic predictions of large numbers of animals in the deep troughs south of Haida Gwaii, an area that had no harbour porpoise sightings during PRISMM or hardly any sightings reported from past DFO cetacean surveys (Ford 2014). Furthermore, model diagnostic plots indicated a great degree of variation in the residuals for the largest depth values, and wide error bands around the linear, positive depth smoother indicated high uncertainty in the relationship the model predicted between water depth and harbour porpoise counts.

The overall Canadian Pacific-wide abundance estimate for harbour porpoises obtained using design-based methods was higher (7,162, Doniol-Valcroze et al., in press) than that produced by the DSM approach (5,207), although both techniques achieved similar levels of precision (total CV = 0.33 for DSM versus 0.38 for design-based). The greater number of porpoises estimated by the design-based approach is in part due to the inclusion of 1,015 individuals estimated for the offshore stratum. Due to the limited number of harbour porpoise sightings in the offshore, a DSM model could not be fit for this stratum and so the overall DSM abundance estimate assumes no harbour porpoises in this region. The 95% CIs of the abundance estimates produced by the two methods were also comparable (2,769-9,793 for DSM versus 3,449-14,871 for design-based).

CONCLUSIONS

Our results complement design-based abundance estimates calculated from the same survey data (Doniol-Valcroze et al., in press), and, when compared with past habitat modelling studies and historic whaling catch data, are useful to inform the extent of recovery of previously harvested populations. The return of these predators to habitats from which they were previously extirpated will have important ecosystem-level implications. The DSM results can also inform management decisions such as Potential Biological Removal limits for fisheries bycatch, as well as providing spatial data that can be used to assess the risk of entanglements, ship strikes, oil spills, acoustic disturbance, and other anthropogenic threats, and can support future Critical Habitat designation and Marine Protected Areas.

ACKNOWLEDGMENTS

We are grateful to the officers and crews of the CCGS *John P. Tully* and the CCGS *Tanu* for their support and efforts during the PRISMM survey. The following individuals provided their expertise as PRISMM marine mammal observers: Robin Abernethy, Jacklyn Barrs, Ali Bowker, Hilary Dennis-Bohm, Thomas Doniol-Valcroze, Caroline Fox, Karen Girouard, Kyla Graham, Anna Hall, Chris Hall, Jackie Hildering, Elise Keppel, Hitomi Kimura, Ashley Kling, Nicole Koshure, Sheena Majewski, Christie McMillan, Kai Meyer, Janet Mossman, Linda Nichol, Alison Ogilvie, Bruce Paterson, Lisa Spaven, and Wendy Szaniszlo. Elizabeth Becker generously provided computer code that we adapted for dividing effort tracklines into equal-sized segments. Mike Foreman, Caroline Fox, Ed Gregr, and Gillian Harvey kindly responded to questions about data sources for environmental covariates. David Miller provided crucial advice and feedback about fitting and validating DSMs.

REFERENCES CITED

Augustin, N.H., Sauleau, E-A., and Wood, S.N. 2012. On quantile quantile plots for generalized linear models. Computational Statistics and Data Analysis 56:2404-2409.

Becker, E.A., Forney, K.A., Ferguson, M.C., Foley, D.G., Smith, R.C., Barlow, J. and Redfern, J.V. 2010. Comparing California Current cetacean-habitat models developed using *in situ* and remotely sensed sea surface temperature data. Marine Ecology Progress Series 413:163-183.

Becker, E.A., Forney, K.A., Miller, D.L., Fiedler, P.C., Barlow, J. and Moore, J.E. 2020. Habitat-based density estimates for cetaceans in the California Current Ecosystem based on 1991-2018 survey data. U.S. Department of Commerce, NOAA Technical Memorandum NMFS-SWFSC-638. 69 pp.

Best, B.D., Fox, C.H., Williams, R.W., Halpin, P.N. and Paquet, P.C. 2015. Updated marine mammal distribution and abundance estimates in British Columbia. Journal of Cetacean Research and Management 15:9-26.

Bouchet, P.J., Meeuwig, J.J., Kent, S., Chandra, P., Letessier, T.B. and Jenner, C.K. 2015. Topographic determinants of mobile vertebrate predator hotspots: current knowledge and future directions. Biological Reviews 90:699-728.

Buckland, S.T., Anderson, D.R., Burnam, K.P., Laake, J.L., Borchers, D.L., and Thomas, L. 2001. Introduction to distance sampling: Estimating abundance of biological populations. Oxford University Press: Oxford, UK.

Calambokidis, J., Falcone, E.A., Quinn, T.J., Burdin, A.M., Clapham, P.J., Ford, J.K.B., Gabriele, C.M., LeDuc, R., Mattila, D., Rojas-Bracho, L., Straley, J.M., Taylor, B.L., Urbán, J.R., Weller, D., Witteveen, B.H., Yamaguchi, M., Bendlin, A., Camacho, D., Flynn, K., Havron, A., Huggins, J. and Maloney, N. 2008. SPLASH: Structure of Populations, Levels of Abundance and Status of Humpback Whales in the North Pacific. Report to U.S. Dept of Commerce, Seattle, Washington. 57 pp.

Croll, D.A., Tershy, B.R., Hewitt, R.P., Demer, D.A., Fiedler, P.C., Smith, S.E., Armstrong, W., Popp, J.M., Kiekhefer, T., Lopez, V.R., Urban, J. and Gendron, D. 1998. An integrated approach to the foraging ecology of marine birds and mammals. Deep-Sea Research II: Topical Studies in Oceanography 45:1353-1371.

Dalla Rosa, L., Ford, J.K.B. and Trites, A.W. 2012. Distribution and relative abundance of humpback whales in relation to environmental variables in coastal British Columbia and adjacent waters. Continental Shelf Research 36:89-104.

DFO. 2009. Development of a framework and principles for the biogeographical classification of Canadian marine areas. DFO Can. Sci. Advis. Sec. Sci. Advis. Rep. 2009/056.

Doniol-Valcroze, T., Nichol, L.M., Wright, B.M., Spaven, L.D., Abernethy, R.M. and Stredulinsky, E.H. Distance sampling abundance estimates of cetaceans from the 2018 Pacific Region International Survey of Marine Megafauna. DFO Can. Sci. Advis. Sec. Res. Doc. In Press.

Dormann, C.F. 2007. Effects of incorporating spatial autocorrelation into the analysis of species distribution data. Global Ecology and Biogeography 16:129-138.

Embling, C.B., Gillibrand, P.A., Gordon, J., Shrimpton, J., Stevick, P.T. and Hammond, P.S. 2010. Using habitat models to identify suitable sites for marine protected areas for harbour porpoises (*Phocoena phocoena*). Biological Conservation 143:267-279.

Fisheries and Oceans Canada. 2013. Recovery Strategy for the North Pacific Humpback Whale (*Megaptera novaeangliae*) in Canada [PROPOSED]. Species at Risk Act Recovery Strategy Series. Fisheries and Oceans Canada, Ottawa. x + 67 pp.

Ford, J.K.B. 2014. Marine Mammals of British Columbia. Royal BC Museum: Victoria, BC.

Ford, J.K.B., Rambeau, A.L., Abernethy, R.M., Boogaards, M.D., Nichol, L.M. and Spaven, L.D. 2009. An assessment of the potential for recovery of humpback whales off the Pacific coast of Canada. DFO Can. Sci. Advis. Sec. Res. Doc. 2009/015. iv + 33 p.

Foreman, M.G.G., Crawford, W.R., Cherniawksy, J.Y., Henry, R.F. and Tarbotton, M.R. 2000. A high-resolution assimilating tidal model for the northeast Pacific Ocean. Journal of Geophysical Research 105(C12):28,629-28,651.

Fox, C.H., Huettmann, F.H., Harvey, G.K.A., Morgan, K.H., Robinson, J., Williams, R. and Paquet, P.C. 2017. Predictions from machine learning ensembles: marine bird distribution and density on Canada’s Pacific coast. Marine Ecology Progress Series 566:199-216.

Hall, A.M. 2004. Seasonal abundance, distribution and prey species of harbour porpoise (*Phocoena phocoena*) in southern Vancouver Island waters. M.Sc. Thesis, University of British Columbia, Vancouver, BC. 100 p.

Hall, A.M. 2011. Foraging behaviour and reproductive season habitat selection of northeast Pacific porpoises. Ph.D. Thesis, University of British Columbia, Vancouver, BC. 185 p.

Harvey, G.K.A., Nelson, T.A., Fox, C.H. and Paquet, P.C. 2017. Quantifying marine mammal hotspots in British Columbia, Canada. Ecosphere 8(7):e01884.

Hijmans, R.J. 2019. Raster: Geographic Data Analysis and Modeling. R package version 2.8-19.

Jefferson, T.A., Smultea, M.A., Courbis, S.S. and Campbell, G.S. 2016. Harbor porpoise (*Phocoena phocoena*) recovery in the inland waters of Washington: estimates of density and abundance from aerial surveys, 2013-2015. Canadian Journal of Zoology 94: 505-515.

Johnston, D.W., Westgate, A.J. and Read, A.J. 2005. Effects of fine-scale oceanographic features on the distribution and movements of harbour porpoises *Phocoena phocoena* in the Bay of Fundy. Marine Ecology Progress Series 295:279-293.

Keen, E. 2017. Aggregative and feeding thresholds of sympatric rorqual whales within a fjord system. Ecosphere 8(3):e01702.

Keen, E.M., Wray, J., Meuter, H. and Thompson, K-L. 2017. 'Whale wave': shifting strategies structure the complex use of critical fjord habitat by humpbacks. Marine Ecology Progress Series 567:211-233.

Keple, A.R. 2002. Seasonal abundance and distribution of marine mammals in the southern Strait of Georgia, British Columbia. M.Sc. Thesis, University of British Columbia, Vancouver, BC. x + 84 p.

Marra, G. and Wood, S.N. 2011. Practical variable selection for generalized additive models. Computational Statistics & Data Analysis 55:2372-2387.

Miller, D.L. 2017. Distance: Distance sampling detection function and abundance estimation. R package version 0.9.7.

Miller, D.L., Burt, M.L., Rexstad, E.A. and Thomas, L. 2013. Spatial models for distance sampling data: recent developments and future directions. Methods in Ecology and Evolution 4:1001-1010.

Miller, D.L., Rexstad, E., Burt, L., Bravington, M.V. and Hedley, S. 2019. dsm: Density Surface Modelling of Distance Sampling Data. R package version 2.2.17. CRAN - Package dsm (r-project.org)

Moran, J.R., O'Dell, M.B, Arimitsu, M.L., Straley, J.M and Dickson, D.M.S. 2018. Seasonal distribution of Dall's porpoise in Prince William Sound, Alaska. Deep Sea Research II 147:164-172.

Nichol, L.M., Abernethy, R.M., Wright, B.M., Heaslip, S., Spaven, L.D., Towers, J.R., Pilkington J.F., Stredulinsky, E.H., and Ford, J.K.B. 2018. Distribution, movements and habitat fidelity patterns of Fin Whales (*Balaenoptera physalus*) in Canadian Pacific Waters. DFO Can. Sci. Advis. Sec. Res. Doc. 2017/004. vii + 52 p.

Nichol, L.M. and Ford, J.K.B. 2012. Information relevant to the assessment of critical habitat for Blue, Fin, Sei and North Pacific Right Whales in British Columbia. DFO Can. Sci. Advis. Sec. Res. Doc. 2011/137. vi + 31 p.

Nichol, L.M., Hall, A.M., Ellis, G.M., Stredulinsky, E., Boogaards, M. and Ford, J.K.B. 2013. Dietary overlap and niche partitioning of sympatric harbour porpoises and Dall's porpoises in the Salish Sea. Progress in Oceanography 115:202-210.

Nichol, L.M., Wright, B.M., O'Hara, P. and Ford, J.K.B. 2017. Risk of lethal vessel strikes to humpback and fin whales off the west coast of Vancouver Island, Canada. Endangered Species Research 32:373-390.

Rogachev, K.A., Carmack, E.C. and Foreman, M.G.G. 2008. Bowhead whales feed on plankton concentrated by estuarine and tidal currents in Academy Bay, Sea of Okhotsk. Continental Shelf Research 28(14):1811-1826.

Springer, A.M., McRoy, C.P. and Flint, M.V. 1996. The Bering Sea Green Belt: Shelf-edge processes and ecosystem production. Fisheries Oceanography 5(3-4):205-223.

Steckler, D., and Donlan, P. 2018. Mysticetus LLC. Version 2.0.

Towers, J.R., Malleson, M., McMillan, C.J., Cogan, J., Berta, S. and Birdsall, C. 2018. Occurrence of fin whales (*Balaenoptera physalus*) between Vancouver Island and continental North America. Northwestern Naturalist 99:49-57.

Turnock, B.J. and Quinn, T.J. 1991. The effect of responsive movement on abundance estimation using line transect sampling. Biometrics 47:701-715.

Wood, S.N. 2017. Generalized Additive Models: An Introduction with R (2nd edition). Chapman and Hall/CRC.

Yen, P.P.W., Sydeman, W.J. and Hyrenback, K.D. 2004. Marine bird and cetacean associations with bathymetric habitats and shallow-water topographies: implications for trophic transfer and conservation. Journal of Marine Systems 50(1-2):79-99.

Zuur, A.F., Ieno, E.N. and Elphick, C.S. 2010. A protocol for data exploration to avoid common statistical problems. Methods in Ecology and Evolution 1:3-14.

TABLES

Table 1. Number of sightings, number of individuals and average group size (± standard deviation) for each species detected visually during the PRISMM survey.

Species	Number of sightings	Number of individuals	Mean group size (±SD)
Humpback whale	767	1145	1.5 (±1.3)
Fin whale	235	357	1.5 (±0.9)
Minke whale	13	14	1.1 (±0.3)
Blue whale	6	10	1.7 (±0.5)
Sei whale	4	5	1.2 (±0.4)
Unidentified large baleen whale	153	188	1.2 (±0.5)
Sperm whale	14	14	1.0 (±0)
Killer whale (all ecotypes)	27	177	6.6 (±4.8)
Pacific white-sided dolphin	25	344	13.8 (±17.9)
Northern right whale dolphin	6	64	10.7 (±16.9)
Risso’s dolphin	4	46	11.5 (±10.7)
Unidentified dolphin	3	13	4.3 (±3.2)
Dall’s porpoise	287	845	2.9 (±1.8)
Harbour porpoise	246	403	1.6 (±0.9)
Unidentified porpoise	24	32	1.3 (±0.9)
Baird’s beaked whale	2	12	6.0 (±0)
Cuvier’s beaked whale	1	5	5.0 (N/A)
Unidentified beaked whale	5	10	2.0 (±1.0)
Unidentified cetacean	52	63	1.2 (±0.6)

Table 2. Best-fit density surface models by species and stratum, showing model covariates (each non-linear term is indicated with a lowercase "s" with the covariate enclosed by parentheses), the response distribution of the best-fit model (Nb=negative binomial, Tw=Tweedie, Qp=quasi-Poisson), and associated abundance estimates with 95% confidence intervals (CI). Coefficient of variation (CV) was calculated using the delta method and is broken into three components, the detection function CV (ddf), the spatial model CV (dsm), and the total CV. For model covariates, the asterisk following a smoother name indicates that a Duchon spline was used instead of a penalized thin plate regression spline.

Species / *Stratum*	Model covariates	Response distribution	Abundance estimate	95% CI	CV ddf	CV dsm	CV total
Humpback whale							
Offshore	s(dst1000m.dir,Y)	Tw	4,935	3,865 – 6,303	0.07	0.10	0.13
North Coast	s(X,Y)	Tw	1,816	1,403 – 2,351	0.07	0.11	0.13
Salish Sea	s(X,Y)	Nb	279	130 – 596	0.07	0.40	0.40
TOTAL			7,030	5,733 – 8,620			0.10
Fin whale							
Offshore	s(X,Y) + s(dst1000m.abs)	Tw	2,732	2,044 – 3,651	0.09	0.12	0.15
North Coast	s(X,Y)	Nb	161	64 – 407	0.09	0.49	0.50
TOTAL			2,893	2,171 – 3,855			0.15
Dall's porpoise							
Offshore	s(dstShore,Y)	Tw	17,934	13,818 – 23,275	0.05	0.12	0.13
North Coast	s(X,Y)	Tw	5,178	3,756 – 7,138	0.05	0.16	0.16
Salish Sea	s(dstShore)*	Tw	580	313 – 1,075	0.05	0.32	0.32
TOTAL			23,692	19,121 – 29,356			0.11
Harbour porpoise							
North Coast	s(X,Y)	Nb	1,314	648 – 2,664	0.28	0.25	0.37
Salish Sea	s(X,Y)	Nb	3,893	1,991 – 7,611	0.28	0.22	0.35
TOTAL			5,207	2,769 – 9,793			0.33

FIGURES

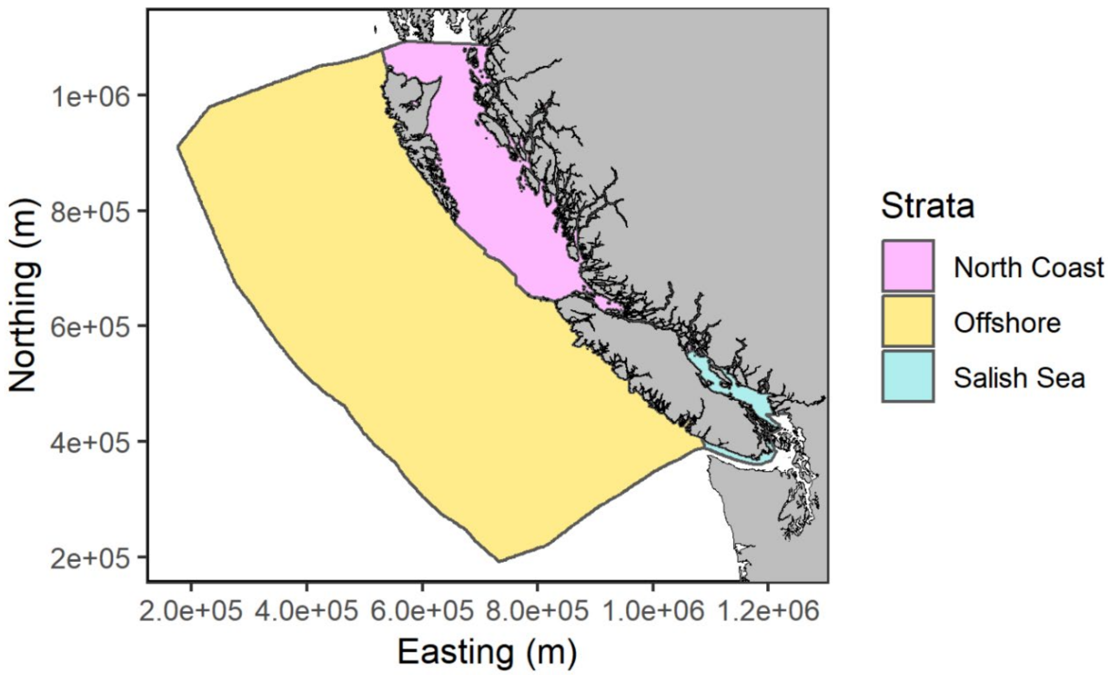

Figure 1. PRISMM study area in British Columbia, Canada, divided into three survey strata: north coast (pink), Salish Sea (blue), and offshore (yellow).

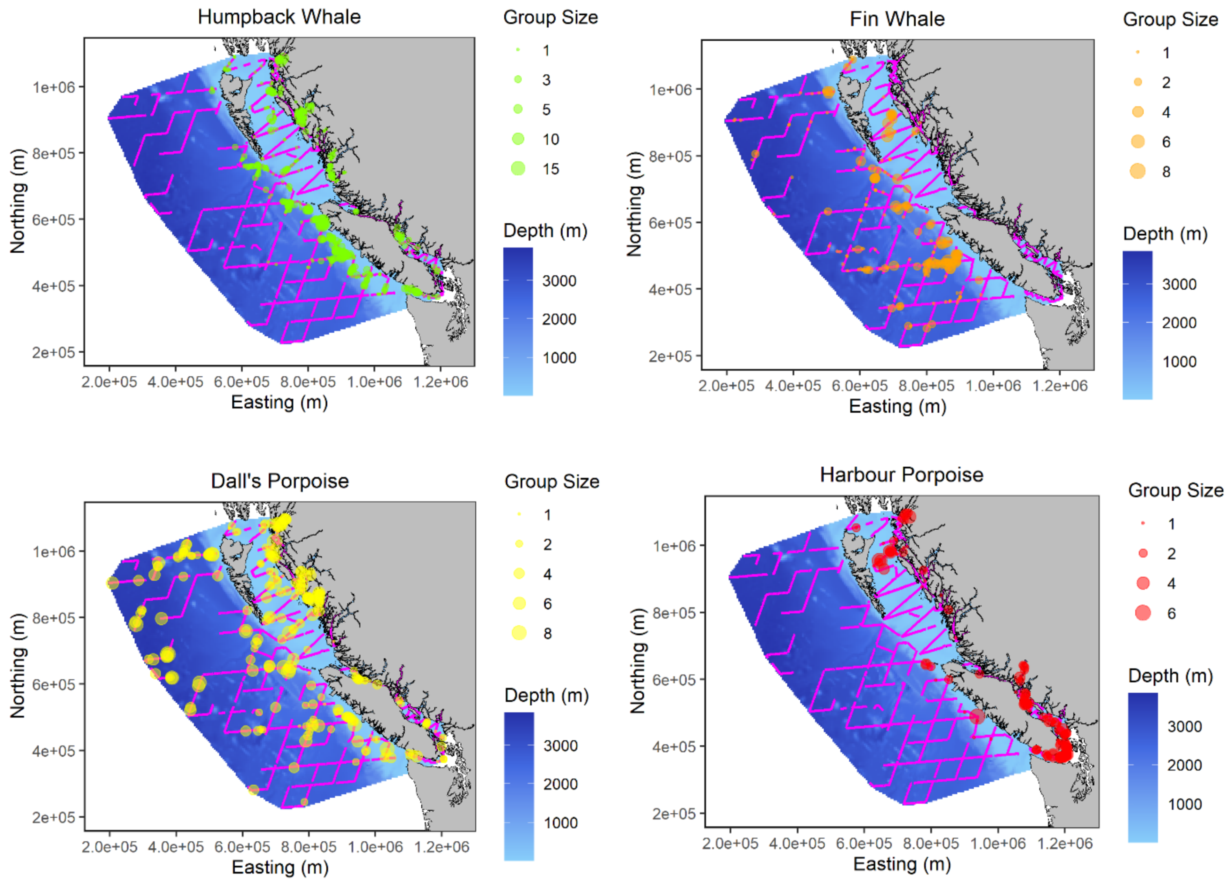

Figure 2. Realized visual on-effort survey tracklines (shown in pink) and sightings (coloured dots) for each species of cetacean for which abundance estimates were generated using DSM. Relative point size within each plot indicates the group size for each sighting. Water depth (m) is indicated by blue shading.

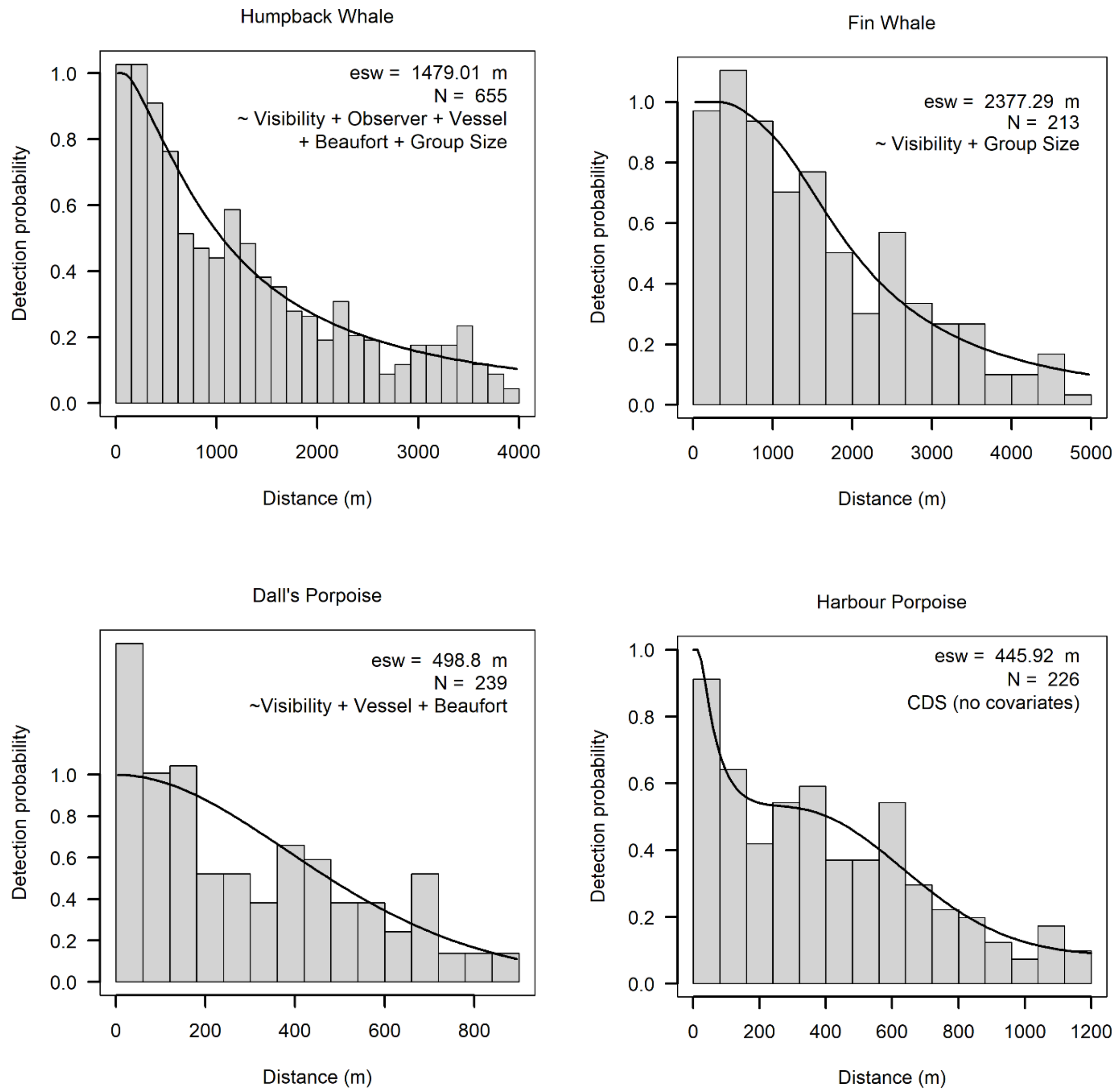

Figure 3. Histograms of observed perpendicular distances and fitted detection functions (DFs) for humpback whale, fin whale, Dall's porpoise and harbour porpoise sightings. All detection functions were fit using the hazard-rate key except for the Dall's porpoise detection function, which used the half-normal key to compensate for the impact of the attractive behaviour of this species to the survey vessel (bow-riding). The effective strip-(half)width (esw), number of sightings (N, after right-truncation), and the formula (covariates) of the best-fit DF model are indicated in the top right corner of each plot. Note that the best-fit harbour porpoise detection function contained no covariates but did include a cosine(2,3) adjustment term.

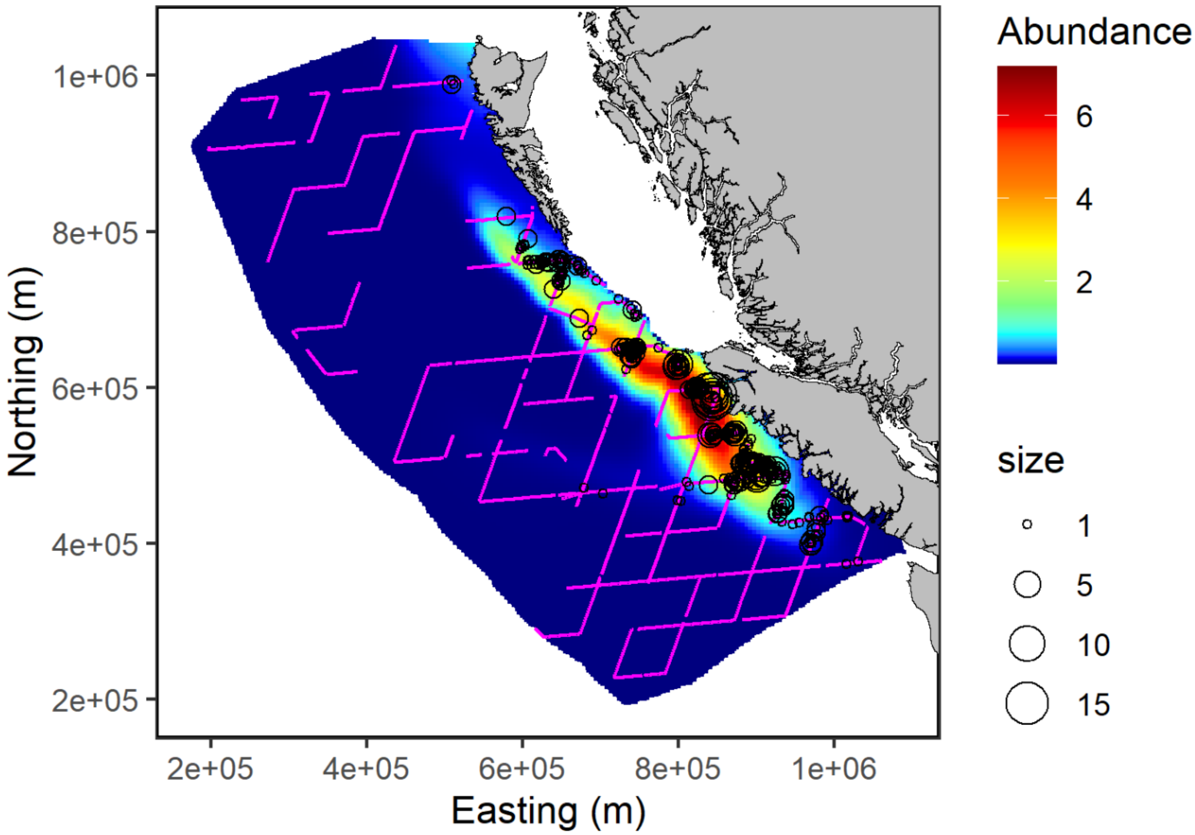

Figure 4. Estimated densities (fill colour indicates the number of individuals per 25 km² grid cell) of humpback whales in the offshore stratum, based on predictions from the best-fit Tweedie GAM. Environmental covariates included in the GAM were distance to the 1,000 m isobath (continental shelf break, measured directionally) and northing (Y coordinates), modelled together as a bivariate smoother. Total estimated abundance for this stratum is 4,935 humpback whales (95% CI = 3,865-6,303). Sighting locations for humpback whales (N = 370) used in the model are indicated by the open circles (group size is denoted by relative circle size). Visual effort track lines are indicated by the magenta lines.

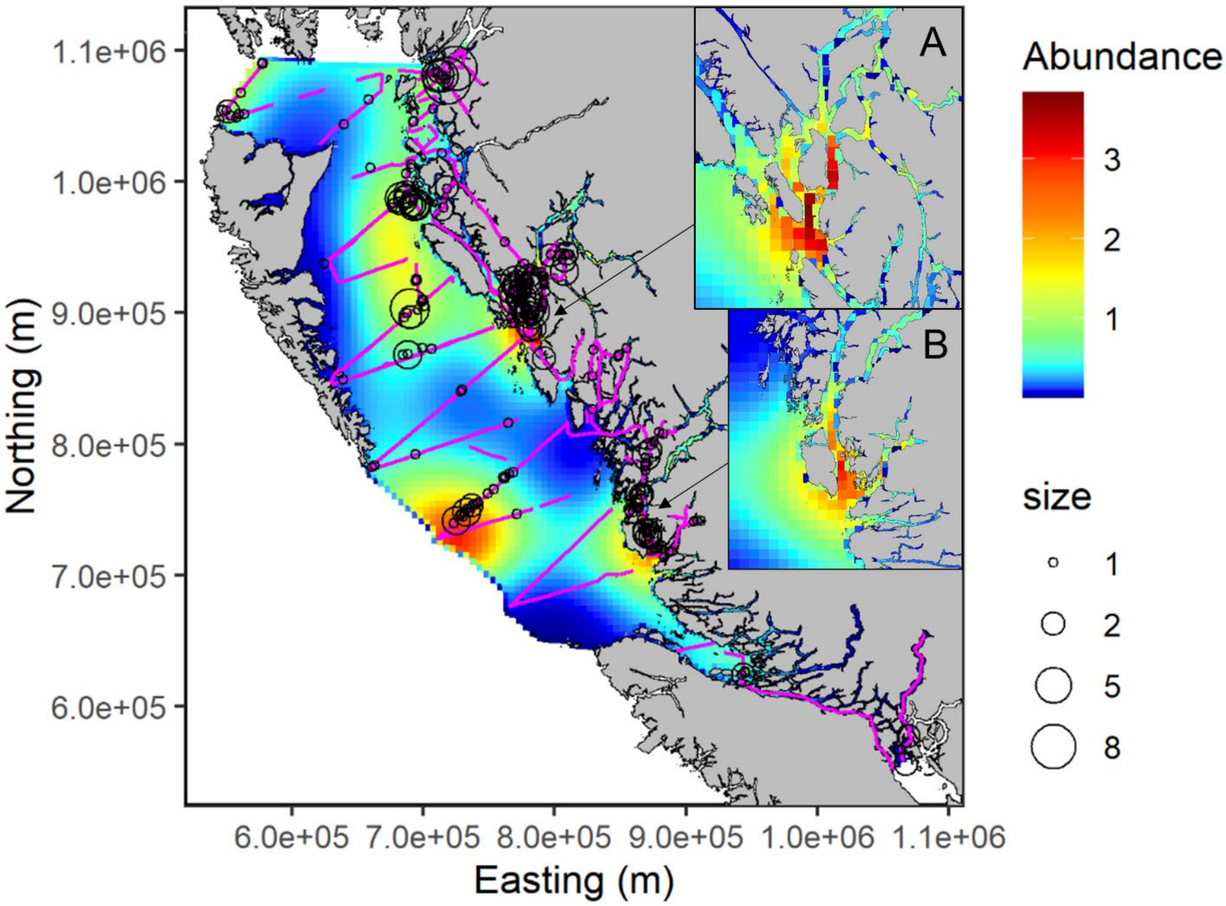

Figure 5. Estimated densities (fill colour indicates the number of individuals per 25 km² grid cell) of humpback whales in the north coast stratum, based on predictions from the best-fit Tweedie GAM. The environmental covariate included in the GAM was a bivariate smoother of easting and northing (X and Y coordinates). Total estimated abundance for this stratum is 1,816 humpback whales (95% CI =1,403-2,351). Sighting locations for humpback whales (N = 263) used in the model are indicated by the open circles (group size is denoted by relative circle size). Visual effort track lines are indicated by the magenta lines. Map insets show details of humpback whale densities predicted in the Caamaño Sound (A) and Fitz Hugh Sound/Rivers Inlet (B) regions.

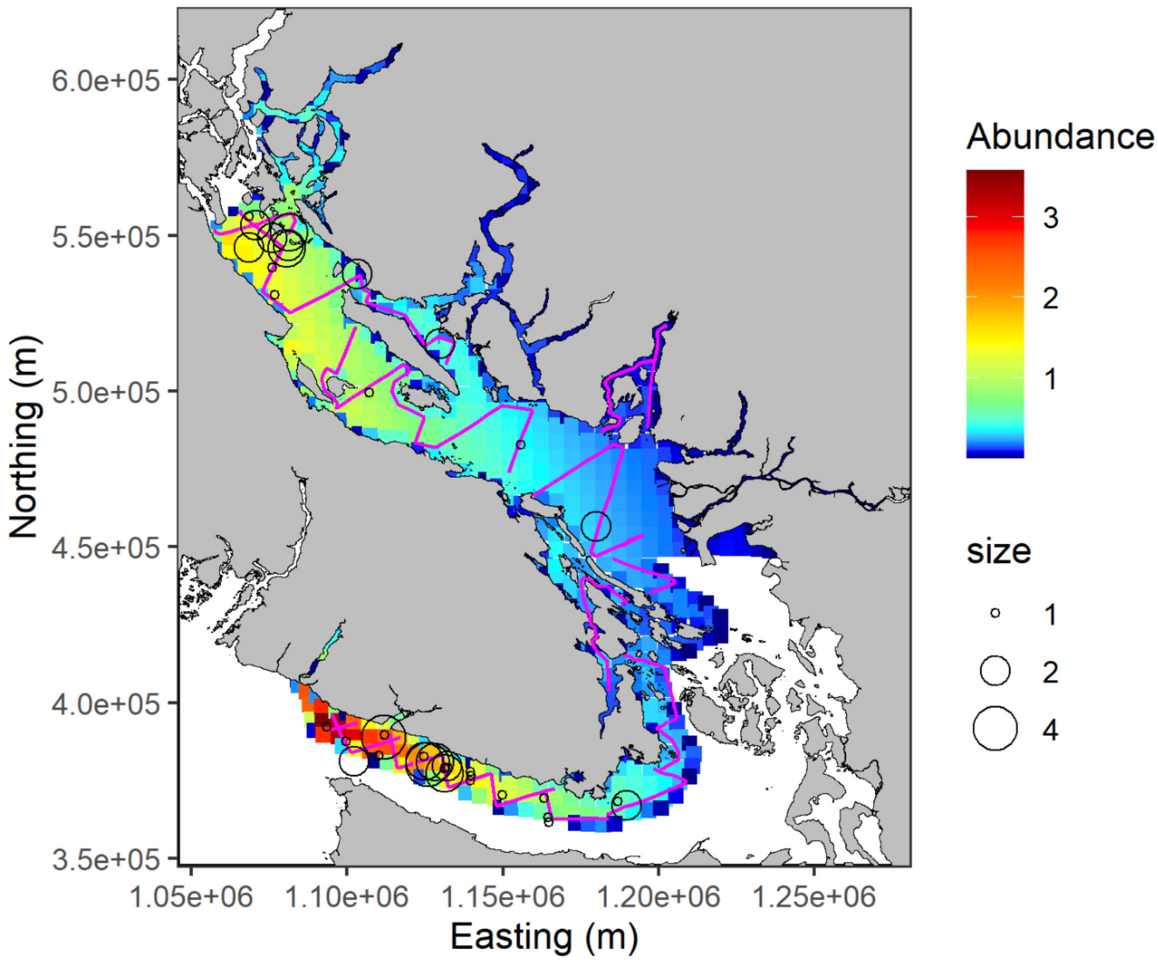

Figure 6. Estimated densities (fill colour indicates the number of individuals per 25 km² grid cell) of humpback whales in the Salish Sea stratum, based on predictions from the best-fit negative binomial GAM. Environmental covariates included in the GAM were a bivariate smoother of easting and northing (X and Y coordinates). Total estimated abundance for this stratum is 279 humpback whales (95% CI = 130-596). Sighting locations for humpback whales (N = 38) used in the model are indicated by the open circles (group size is denoted by relative circle size). Visual effort track lines are indicated by the magenta lines.

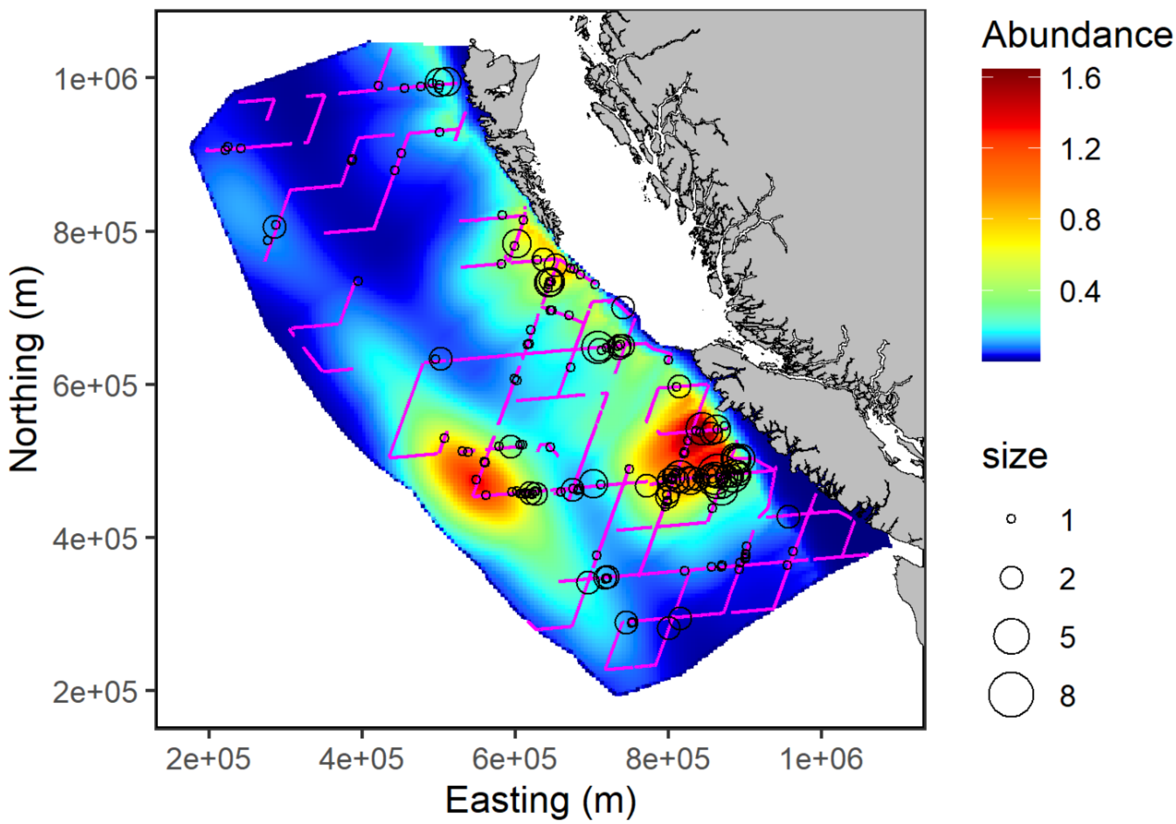

Figure 7. Estimated densities (fill colour indicates the number of individuals per 25 km^2 grid cell) of fin whales in the offshore stratum, based on predictions from the best-fit Tweedie GAM. Environmental covariates included in the GAM were a bivariate smoother of easting and northing (X and Y coordinates), and a smoother of distance (absolute values) to the 1,000 m isobath. Total estimated abundance for this stratum is 2,732 fin whales (95% CI =2,044-3,651). Sighting locations for fin whales (N = 184) used in the model are indicated by the open circles (group size is denoted by relative circle size). Visual effort track lines are indicated by the magenta lines.

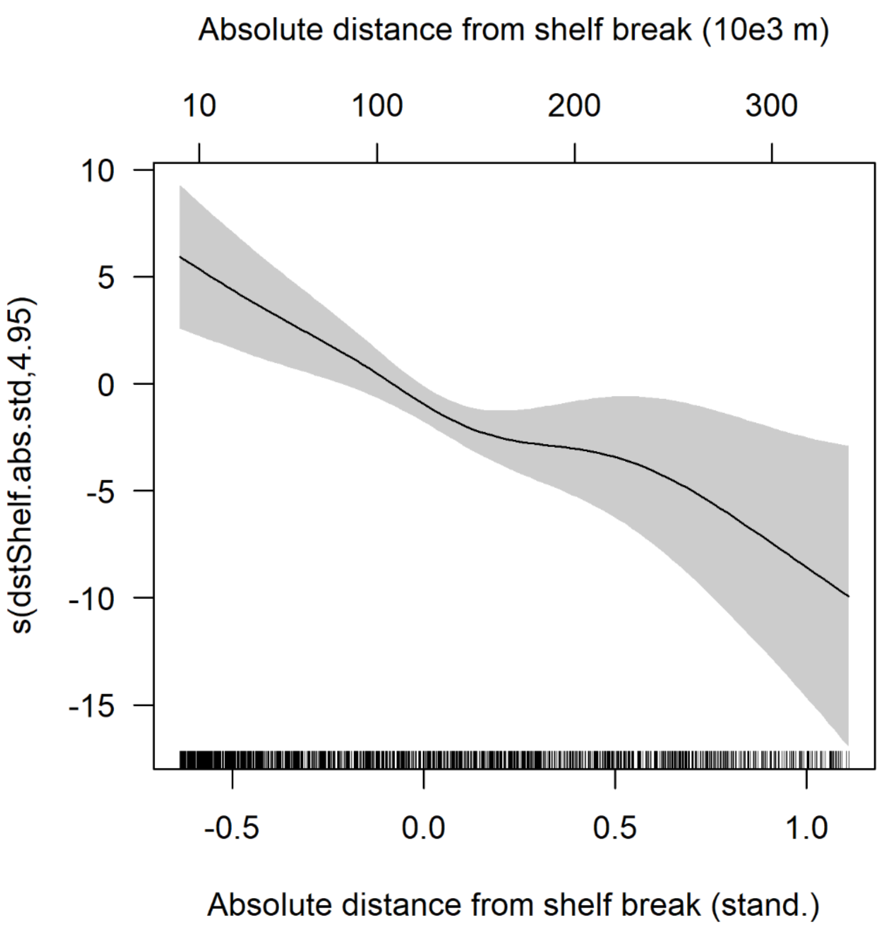

Figure 8. Smoothing function (solid line) with 95% CIs (shaded bands) of distance from shelf break (1,000 m contour, calculated as absolute values) from the top-ranked DSM for fin whales in the offshore stratum (edf = 4.95). Rug plot along lower x-axis indicates the distribution of sampled values within the distance to shelf break covariate. For ease of interpretation, unstandardized values (in 10^3 m) of the covariate are shown along the upper x-axis.

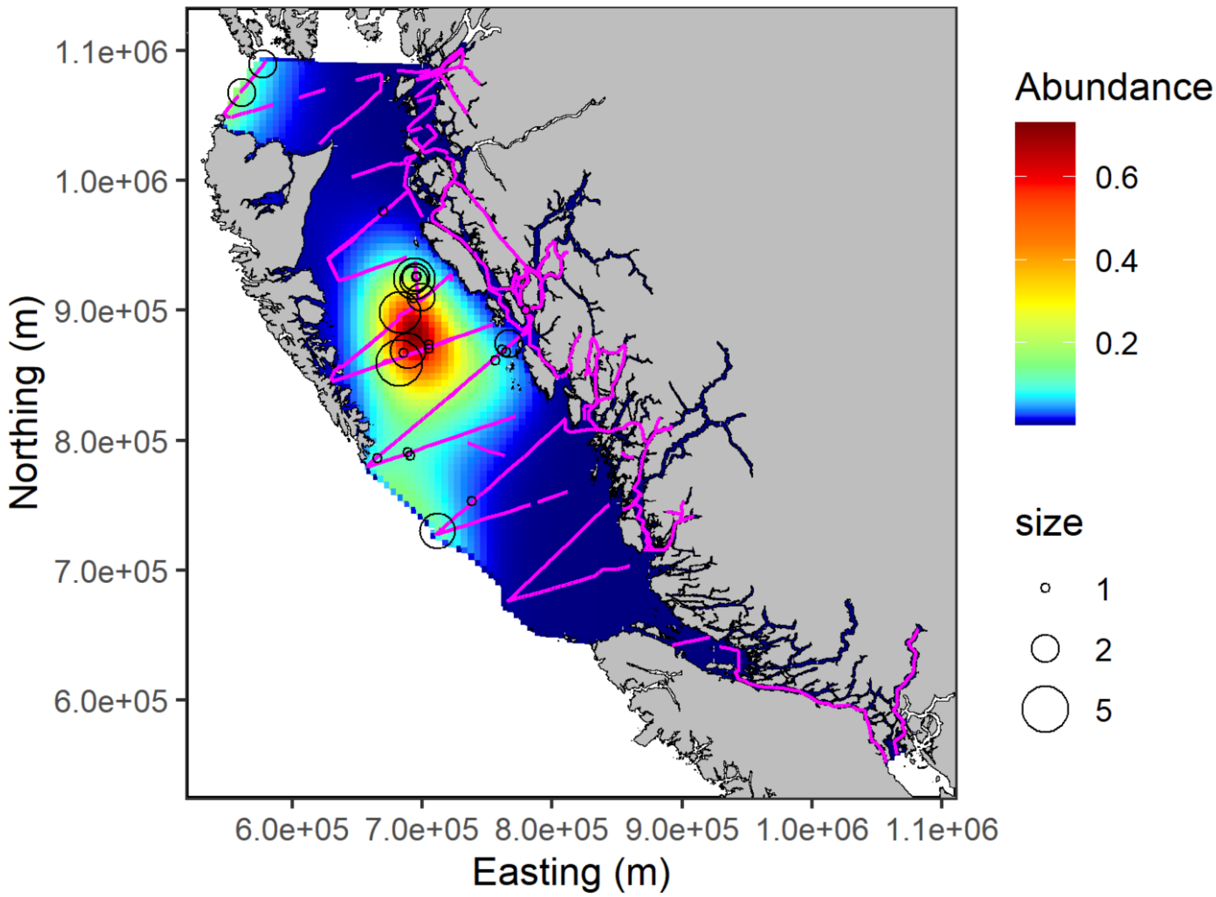

Figure 9. Estimated densities (fill colour indicates the number of individuals per 25 km² grid cell) of fin whales in the north coast stratum, based on predictions from the best-fit negative binomial GAM. The environmental covariate included in the GAM was a bivariate smoother of easting and northing (X and Y coordinates). Total estimated abundance for this stratum is 161 fin whales (95% CI =64-407). Sighting locations for fin whales (N = 29) used in the model are indicated by the open circles (group size is denoted by relative circle size). Visual effort track lines are indicated by the magenta lines.

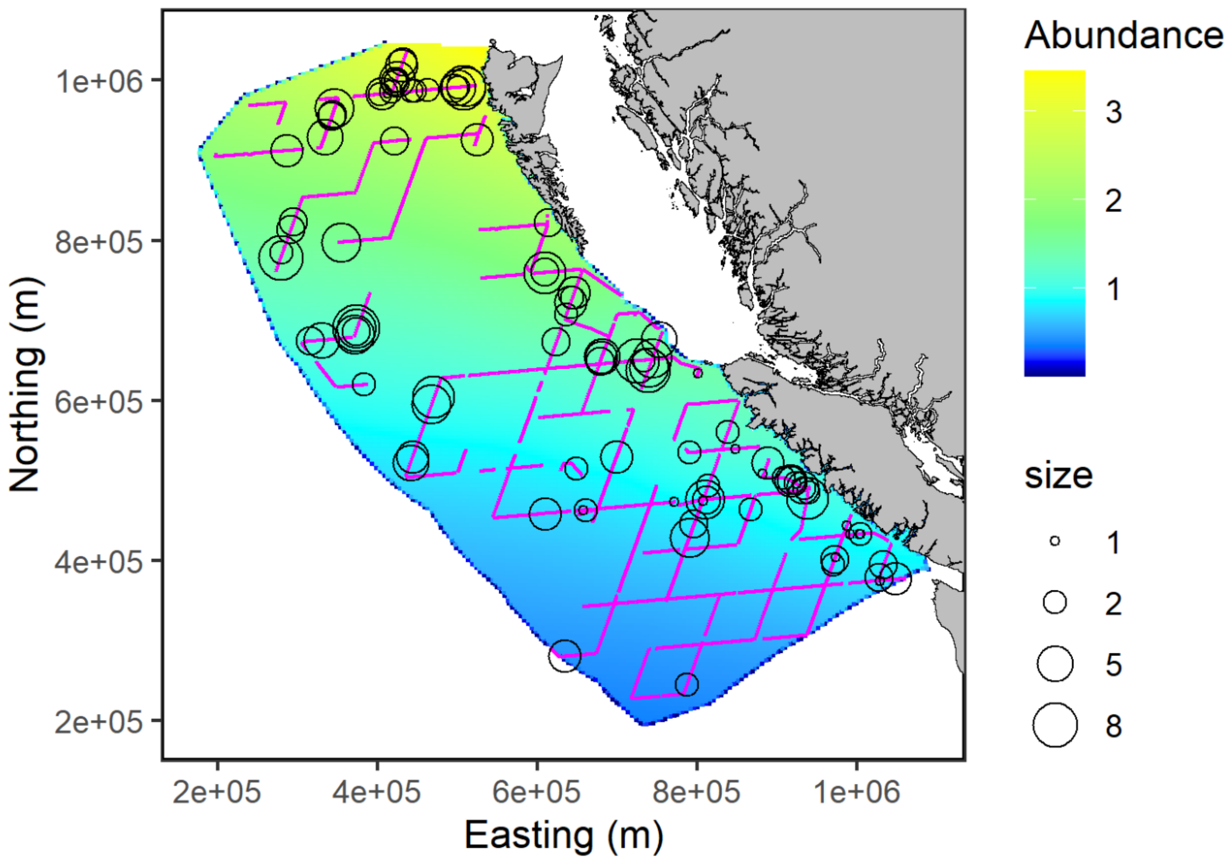

Figure 10. Estimated densities (fill colour indicates the number of individuals per 25 km^2 grid cell) of Dall's porpoises in the offshore stratum, based on predictions from the best-fit Tweedie GAM. The environmental covariate included in the GAM was a bivariate smoother of distance from shore and northing (Y coordinates). Total estimated abundance for this stratum is 17,934 Dall's porpoises (95% CI = 13,818-23,275). Sighting locations for Dall's porpoises (N = 100) are indicated by the open circles (group size is denoted by relative circle size). Visual effort track lines are indicated by the magenta lines.

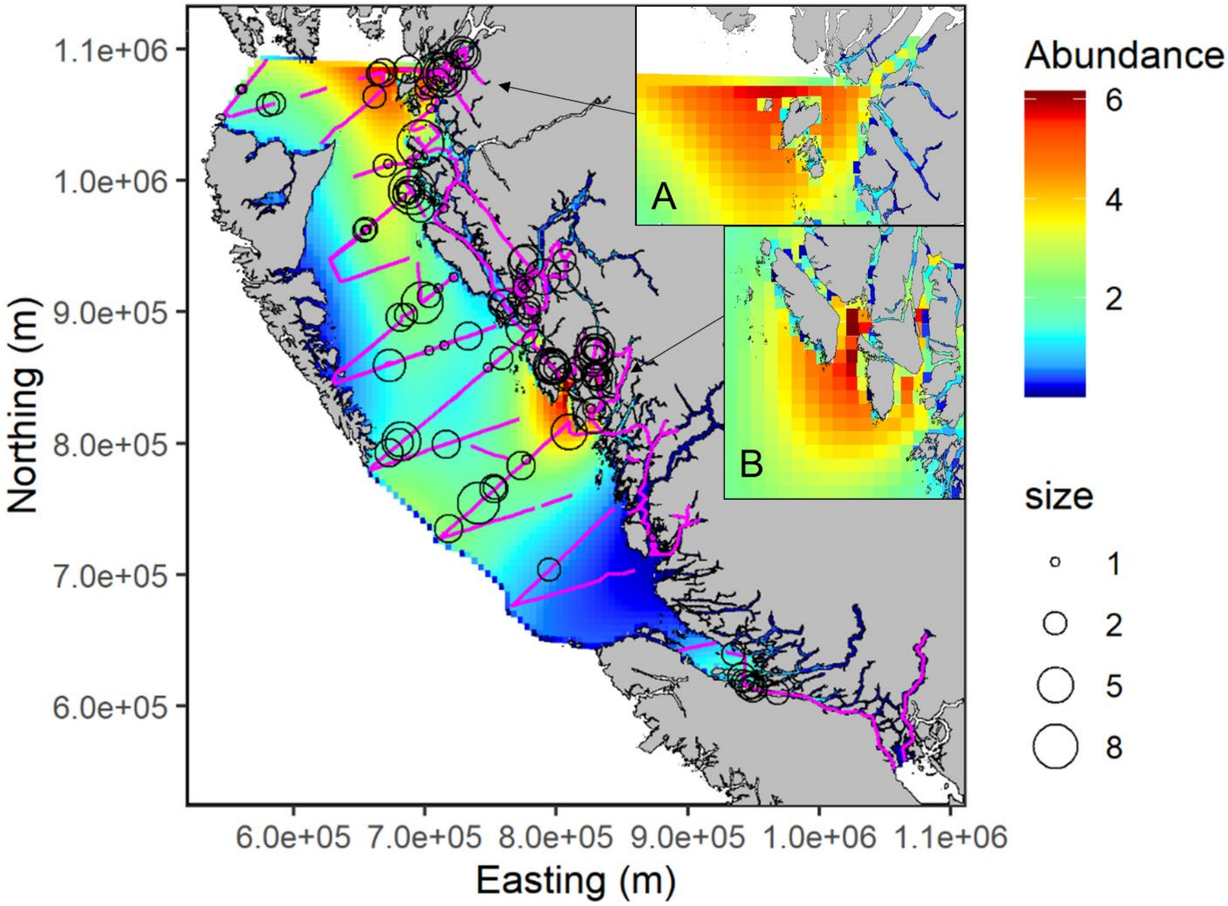

Figure 11.[1] *Estimated densities (fill colour indicates the number of individuals per 25 km² grid cell) of Dall's porpoises in the north coast stratum, based on predictions from the best-fit Tweedie GAM. Environmental covariates included in the GAM were a bivariate smoother of easting and northing (X and Y coordinates). Total estimated abundance for this stratum is 5,178 Dall's porpoises (95% CI =3,756-7,138). Sighting locations for Dall's porpoises (N = 112) are indicated by the open circles (group size is denoted by relative circle size). Visual effort track lines are indicated by the magenta lines. Map insets show details of Dall's porpoise densities predicted in the Portland Inlet/Chatham Sound (A) and Laredo Sound/Milbanke Sound (B) regions.*

[1] Erratum: Figure 11 was a duplicate of Figure 5, and now shows the correct figure.

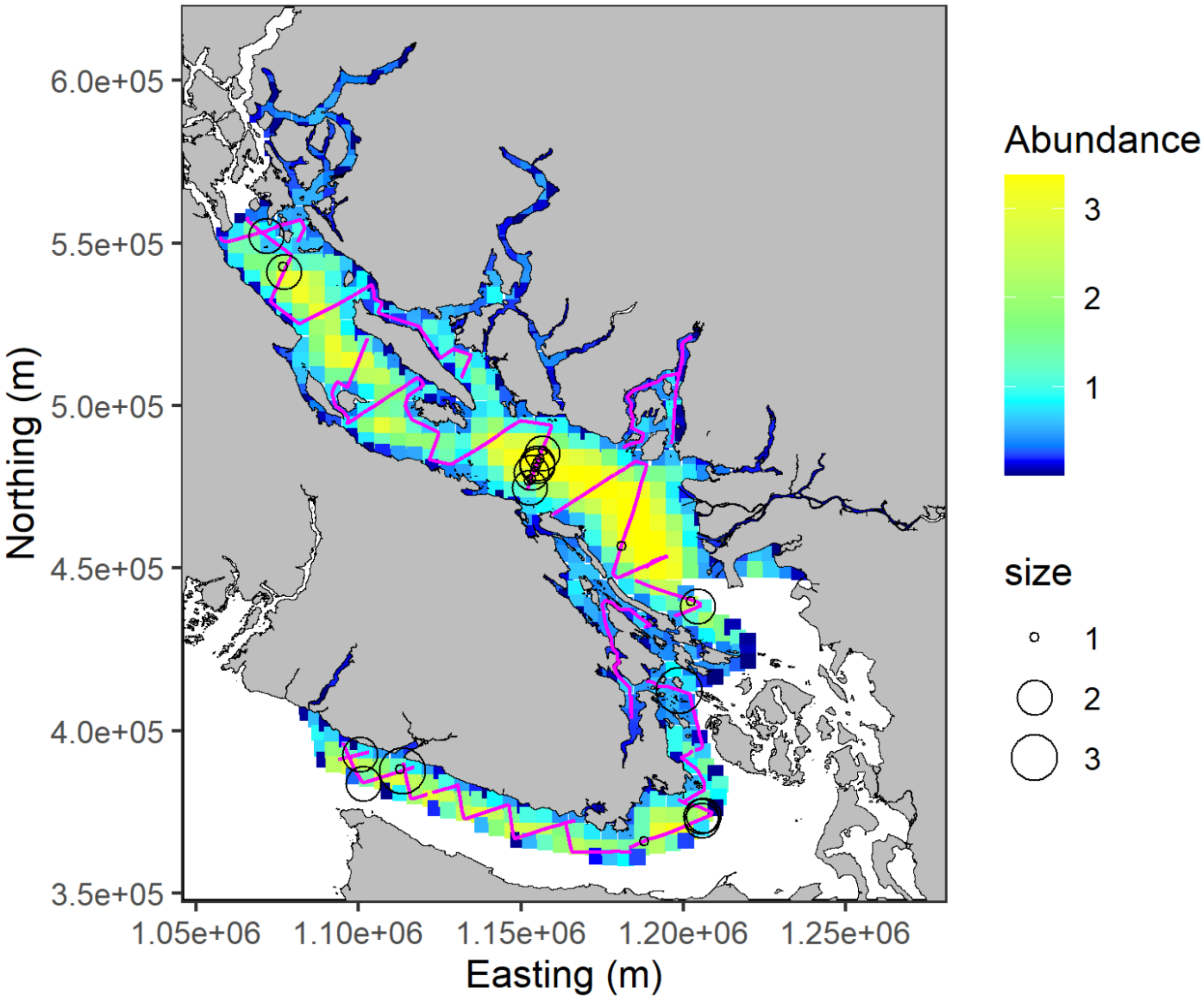

Figure 12. Estimated densities (fill colour indicates the number of individuals per 25 km² grid cell) of Dall's porpoises in the Salish Sea stratum, based on predictions from the best-fit Tweedie GAM. The only significant environmental covariate included in the GAM was a smoother of distance from nearest shore (Duchon spline). Total estimated abundance for this stratum is 580 Dall's porpoises (95% CI = 313-1,075). Sighting locations for Dall's porpoises (N = 27) are indicated by the open circles (group size is denoted by relative circle size). Visual effort track lines are indicated by the magenta lines.

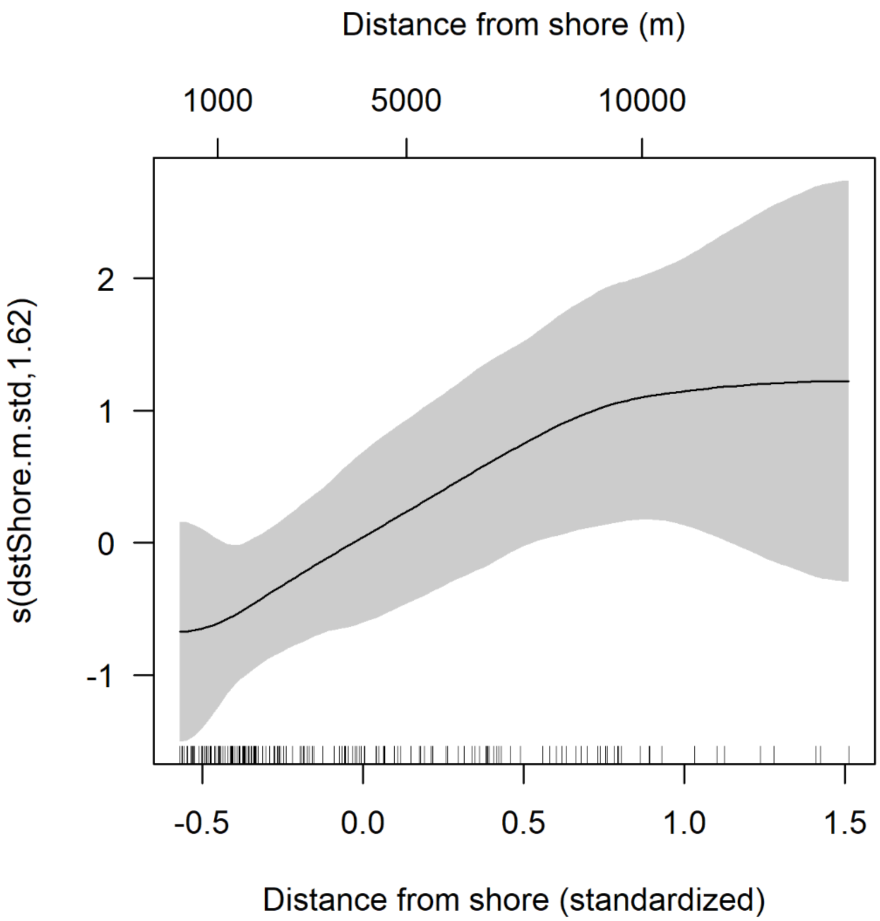

Figure 13. Smoothing function (solid line, Duchon spline) with 95% CIs (shaded band) of distance from nearest shore from the top-ranked DSM for Dall's porpoise in the Salish Sea stratum (edf = 1.62). Rug plot along lower x-axis indicates the distribution of sampled values within the distance from shore covariate. For ease of interpretation, unstandardized values (m) of the covariate are shown along the upper x-axis.

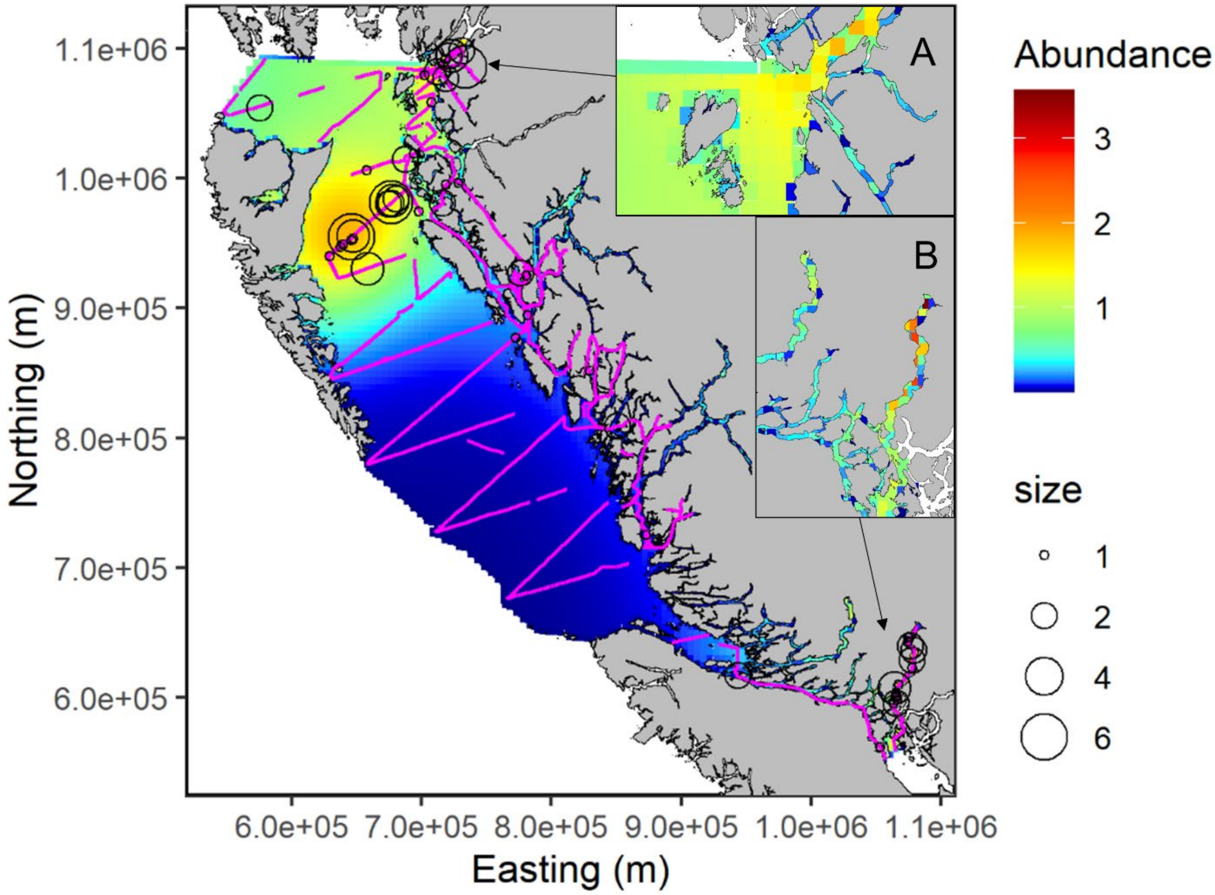

Figure 14. Estimated densities (fill colour indicates the number of individuals per 25 km² grid cell) of harbour porpoises in the north coast stratum, based on predictions from the best-fit negative binomial GAM. The only significant environmental covariates included in the GAM was a bivariate smoother of easting and northing (X and Y coordinates). Total estimated abundance for this stratum is 1,314 harbour porpoises (95% CI = 648-2,664). Sighting locations for harbour porpoises (N = 54) used in the model are indicated by the open circles (group size is denoted by relative circle size). Visual effort track lines are indicated by the magenta lines. Map insets show details of harbour porpoise densities predicted in the Portland Inlet/Chatham Sound (A) and Knight/Bute Inlet (B) regions.

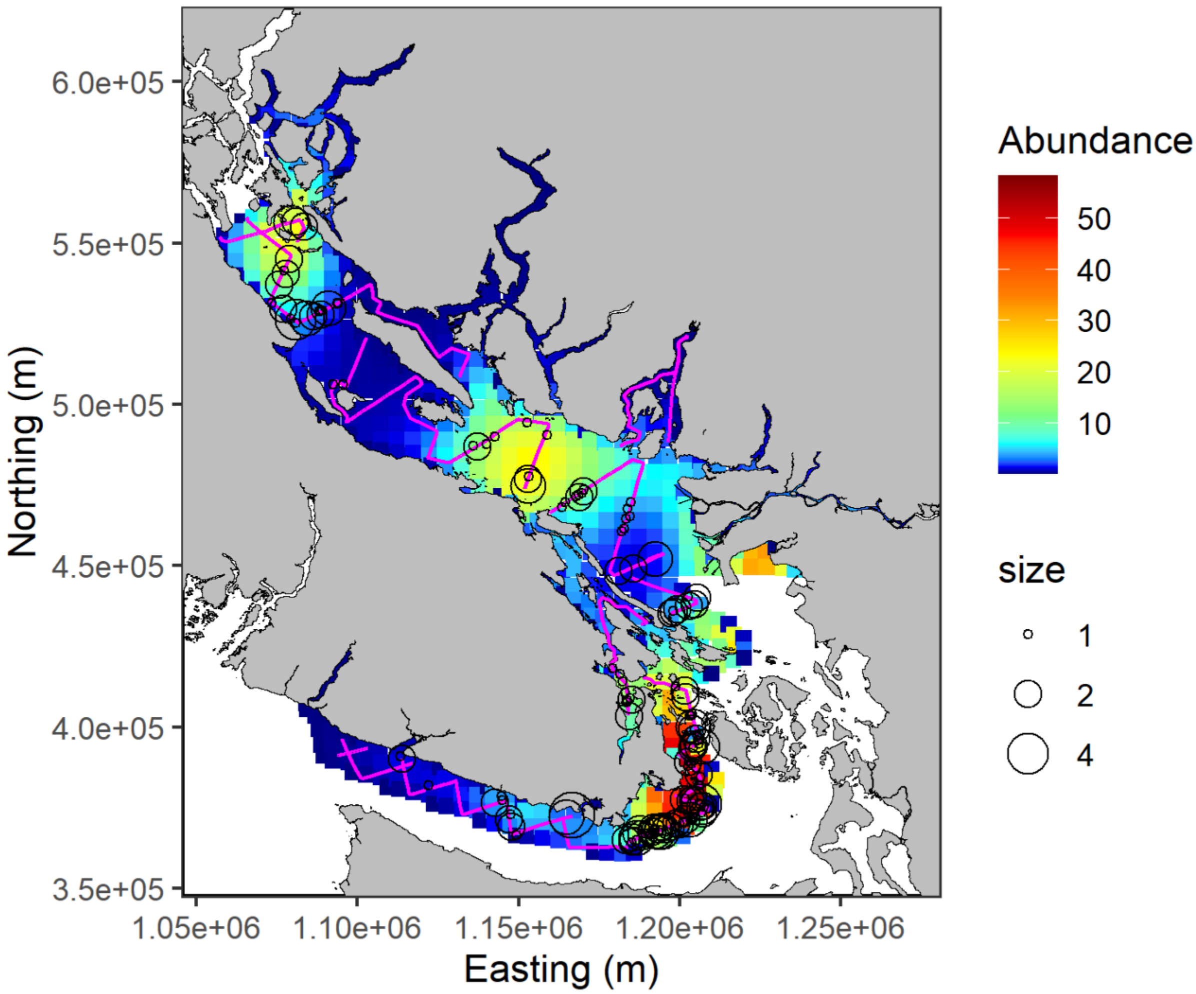

Figure 15. Estimated densities (fill colour indicates the number of individuals per 25 km^2 grid cell) of harbour porpoises in the Salish Sea stratum, based on predictions from the best-fit negative binomial GAM. The only significant environmental covariates included in the GAM was a bivariate smoother of easting and northing (X and Y coordinates). Total estimated abundance for this stratum is 3,893 harbour porpoises (95% CI = 1,991-7,611). Sighting locations for harbour porpoises (N = 161) used in the model are indicated by the open circles (group size is denoted by relative circle size). Visual effort track lines are indicated by the magenta lines.

APPENDIX A. CANDIDATE DENSITY SURFACE MODELS

Table A1. Candidate DSMs for humpback whales in the offshore survey stratum, including response distributions (Qp=quasiPoisson, Nb=negative binomial, Tw=Tweedie), deltaAIC values (within each response distribution), and dispersion statistics (values >1 indicate overdispersion and <1 indicate underdispersion). Non-linear smoother terms are enclosed in the notation 's( )' and the effective degrees of freedom of each term are also noted within the brackets. Models are listed in ascending order of deltaAIC within each response distribution and the selected best-fit model is highlighted in bold font.

Model covariates	Response distribution	deltaAIC	Estimated abundance	Dispersion statistic
s(dst1000m.dir,Y, 17.4)	Nb	0	4,930	0.49
s(dst1000m.abs,Y, 15.7)	Nb	1.9	23,656	0.51
s(dst1000m.zero,Y, 16.5)	Nb	5.6	13,431	0.41
s(X,Y, 16.7) + s(dst1000m.abs, 1.3)	Nb	14.4	48,410	0.61
s(dst200m.abs,Y, 14.3)	Nb	18.1	11,849	0.60
s(dst200m.dir,Y, 15.1)	Nb	20.2	6,126	0.62
s(X,Y, 15.9) + s(dst1000m.zero, 1.7)	Nb	26.2	22,512	0.67
s(dst200m.zero,Y, 14.4)	Nb	32.4	9,004	0.59
s(X,Y, 11.6) + s(dst200.abs, 1.8)	Nb	38.2	12,600	0.85
s(X,Y, 10.4) + s(dst200.zero, 2.1)	Nb	41.1	9,281	0.90
s(X,Y, 10.1) + s(dst200.dir, 4.7)	Nb	42.5	4,755	0.76
s(dstShore,Y, 14.5)	Nb	42.7	5,646	0.58
s(X,Y, 9.4) + s(dstShore, 4.0)	Nb	51.6	5,416	0.78
s(X,Y, 11.2) + s(depth, 2.8)	Nb	59.6	10,798	0.67
s(X,Y, 13.6)	Nb	65.8	12,299	0.76
s(X,Y, 15.5) + s(dst1000m.abs, 1.3)	Tw	0	33,673	3.01
s(dst1000m.dir,Y, 17.5)	**Tw**	**1.4**	**4,935**	**2.42**
s(X,Y, 9.2) + s(depth, 0.8) + s(dst200.abs, 2.1)	Tw	2.6	13,043	5.41
s(dst200m.dir,Y, 14.8)	Tw	5.6	5,554	2.94
s(X,Y, 9.4) + s(dst200m.dir, 5.0)	Tw	6.0	4,559	3.73
s(X,Y, 15.1) + s(dst1000m.dir, 5.7)	Tw	6.2	4,935	2.67
s(X,Y, 20.8)	Tw	6.2	8,768	2.45
s(X,Y, 9.2) + s(depth, 2.8) + s(dst200m.zero, 1.8)	Tw	6.9	9,419	4.37
s(dst1000m.abs,Y, 14.5)	Tw	7.3	16,078	2.67
s(dst200m.abs,Y, 12.8)	Tw	7.5	9,943	3.12
s(X,Y, 14.8) + s(dst1000m.zero, 1.7)	Tw	8.8	18,727	3.43
s(X,Y, 10.9) + s(depth, 4.3) + s(dstShore, 1.2)	Tw	14.5	8,527	3.51
s(dst1000m.zero,Y, 16.1)	Tw	14.6	11,086	2.25
s(dst200m.zero,Y, 14.3)	Tw	15.4	7,460	2.94
s(dstShore,Y, 14.7)	Tw	24.2	5,388	2.89
s(X,Y, 25.1)	Qp	N/A	9,184	2.15

Table A2. Candidate DSMs for humpback whales in the north coast survey stratum, including response distributions (Qp=quasiPoisson, Nb=negative binomial, Tw=Tweedie), deltaAIC values (within each response distribution), and dispersion statistics (values >1 indicate overdispersion and <1 indicate underdispersion). Non-linear smoother terms are enclosed in the notation 's( )' and the effective degrees of freedom of each term are also noted within the brackets. Models are listed in ascending order of deltaAIC within each response distribution and the selected best-fit model is highlighted in bold font. Only one of the negative binomial models tested contained significant terms, and therefore no deltaAIC values are shown for this response distribution.

Model covariates	Response distribution	deltaAIC	Estimated abundance	Dispersion statistic
s(depth, 0.9) + s(dstShore, 2.5)	Nb	N/A	2,255	0.69
s(X,Y, 23.6) + s(TidalSpd, 3.7) + s(dstHTidal, 0.8)	Tw	0	1,833	6.59
s(X,Y, 24.0)	**Tw**	**1.7**	**1,816**	**7.03**
s(X,Y, 26.4)	Qp	N/A	1,886	7.73

Table A3. Candidate DSMs for humpback whales in the Salish Sea survey stratum, including response distributions (Qp=quasiPoisson, Nb=negative binomial, Tw=Tweedie), deltaAIC values (within each response distribution), and dispersion statistics (values >1 indicate overdispersion and <1 indicate underdispersion). Non-linear smoother terms are enclosed in the notation 's( )' and the effective degrees of freedom of each term are also noted within the brackets. Models are listed in ascending order of deltaAIC within each response distribution and the selected best-fit model is highlighted in bold font.

Model covariates	Response distribution	deltaAIC	Estimated abundance	Dispersion statistic
s(X,Y, 2.5) + s(dstShore, 1.0)	Nb	0	918	0.58
s(X,Y, 1.9)	**Nb**	**15.4**	**279**	**1.61**
s(X,Y, 2.8) + s(dstShore, 6.5)	Tw	0	1,011,245	2.44
s(X,Y, 2.4)	Tw	16.5	330	18.23
s(X,Y, 13.1)	Qp	N/A	321	5.20

Table A4. Candidate DSMs for fin whales in the offshore survey stratum, including response distributions (Qp=quasiPoisson, Nb=negative binomial, Tw=Tweedie), deltaAIC values (within each response distribution), and dispersion statistics (values >1 indicate overdispersion and <1 indicate underdispersion). Non-linear smoother terms are enclosed in the notation 's( )' and the effective degrees of freedom of each term are also noted within the brackets. Models are listed in ascending order of deltaAIC within each response distribution and the selected best-fit model is highlighted in bold font.

Model covariates	Response distribution	deltaAIC	Estimated abundance	Dispersion statistic
s(dst1000m.dir,Y, 21.2)	Nb	0	2,174	0.69
s(dst200m.dir,Y, 21.3)	Nb	1.7	2,222	0.67
s(X,Y, 13.9) + s(dst1000m.abs, 4.6)	Nb	6.0	2,417	0.68
s(dst200m.zero,Y, 20.5)	Nb	9.7	2,236	0.69
s(dstShore,Y, 20.6)	Nb	10.6	2,212	0.69
s(X,Y, 14.4) + s(dst1000m.zero, 4.5)	Nb	10.9	2,172	0.68
s(dst1000m.zero,Y, 19.8)	Nb	13.7	2,184	0.69
s(X,Y, 18.1) + s(depth, 2.2)	Nb	16.4	2,454	0.69
s(X,Y, 15.4) + s(depth, 0.9) + s(dst200m.abs, 4.1)	Nb	16.8	2,338	0.69
s(dst200m.abs,Y, 19.4)	Nb	19.8	2,228	0.67
s(X,Y, 18.4)	Nb	22.9	2,168	0.67
s(dst1000m.abs,Y, 18.5)	Nb	23.0	2,374	0.66
s(X,Y, 17.0) + s(dst1000m.abs, 5.0)	**Tw**	**0**	**2,732**	**3.34**
s(dst1000m.dir,Y, 23.5)	Tw	0.3	2,427	3.21
s(dst200m.dir,Y, 23.3)	Tw	0.7	2,496	3.20
s(X,Y, 21.6)	Tw	1.1	2,474	3.41
s(X,Y, 20.3) + s(depth, 2.7)	Tw	2.2	2,890	3.31
s(dst200.zero,Y, 22.6)	Tw	2.3	2,506	3.36
s(dstShore,Y, 22.1)	Tw	2.4	2,445	3.47
s(dst1000m.zero,Y, 22.4)	Tw	3.2	2,435	3.50
s(dst200m.abs,Y, 22.4)	Tw	4.4	2,503	3.55
s(X,Y, 16.4) + s(depth, 2.3) + s(dst1000m.zero, 5.0)	Tw	4.7	2,827	3.44
s(dst1000m.abs,Y, 21.9)	Tw	6.4	2,673	3.53
s(X,Y, 18.0) + s(depth, 2.5) + s(dst200m.abs, 4.9)	Tw	7.7	2,879	3.30
s(X,Y, 18.4) + s(depth,2.5) + s(dstShore, 4.8)	Tw	8.0	2,826	3.30
s(X,Y, 25.6)	Qp	N/A	2,471	3.05

Table A5. Candidate DSMs for fin whales in the north coast survey stratum, including response distributions (Qp=quasiPoisson, Nb=negative binomial, Tw=Tweedie), and dispersion statistics (values >1 indicate overdispersion and <1 indicate underdispersion). Non-linear smoother terms are enclosed in the notation 's( )' and the effective degrees of freedom of each term are also noted within the brackets. The selected best-fit model is highlighted in bold font. Values of deltaAIC were not calculated for this model set, as there was only one candidate model within each of the response distributions tested.

Model covariates	Response distribution	deltaAIC	Estimated abundance	Dispersion statistic
s(X,Y, 10.7)	**Nb**	**N/A**	**161**	**0.25**
s(X,Y, 12.9)	Tw	N/A	237	1.97
s(X,Y, 19.5)	Qp	N/A	304	0.92

Table A6. Candidate DSMs for Dall's porpoises in the offshore survey stratum, including response distributions (Qp=quasiPoisson, Nb=negative binomial, Tw=Tweedie), deltaAIC values (within each response distribution), and dispersion statistics (values >1 indicate overdispersion and <1 indicate underdispersion). Non-linear smoother terms are enclosed in the notation 's( )' and the effective degrees of freedom of each term are also noted within the brackets. Models are listed in ascending order of deltaAIC within each response distribution and the selected best-fit model is highlighted in bold font.

Model covariates	Response distribution	deltaAIC	Estimated abundance	Dispersion statistic
s(dstShore,Y, 1.7)	Nb	0	17,341	0.51
s(dst200m.dir,Y, 1.8)	Nb	0	17,316	0.51
s(dst1000m.dir,Y, 1.8)	Nb	0.1	17,323	0.51
s(dst200m.zero,Y, 1.8)	Nb	0.1	17,322	0.51
s(dst200m.abs,Y, 1.7)	Nb	0.3	17,326	0.50
s(dst1000m.zero,Y, 1.8)	Nb	0.3	17,318	0.50
s(X,Y, 1.5)	Nb	0.3	17,382	0.49
s(dst1000m.abs,Y, 1.7)	Nb	0.5	17,313	0.50
s(dstShore,Y, 2.1)	**Tw**	**0**	**17,934**	**9.95**
s(dst200m.abs,Y, 10.8)	Tw	6.0	17,394	8.31
s(dst200m.dir,Y, 10.8)	Tw	6.1	17,126	8.38
s(dst200m.zero,Y, 11.2)	Tw	6.5	17,313	8.27
s(X,Y, 10.5)	Tw	6.5	17,303	8.50
s(dst1000m.abs,Y, 11.5)	Tw	6.8	16,748	7.95
s(dst1000m.zero,Y, 11.5)	Tw	6.8	16,913	8.10
s(dst1000m.dir,Y, 11.9)	Tw	8.3	16,693	8.08
s(X,Y, 9.2) + s(dst200m.dir, 1.4)	Tw	8.6	15,859	8.58
s(X,Y, 25.7)	Qp	N/A	19,259	5.42

Table A7. Candidate DSMs for Dall's porpoises in the north coast survey stratum, including response distributions (Qp=quasiPoisson, Nb=negative binomial, Tw=Tweedie), deltaAIC values (within each response distribution), and dispersion statistics (values >1 indicate overdispersion and <1 indicate underdispersion). Non-linear smoother terms are enclosed in the notation 's( )' and the effective degrees of freedom of each term are also noted within the brackets. Models are listed in ascending order of deltaAIC within each response distribution and the selected best-fit model is highlighted in bold font. None of the negative binomial models that were tested contained any significant covariates, and so they are not shown here. The notation ~1 denotes a null model with no covariate terms.

Model covariates	Response distribution	deltaAIC	Estimated abundance	Dispersion statistic
s(X,Y, 15.9)	**Tw**	**0**	**5,178**	**7.14**
~ 1	Tw	2.4	5,659	11.84
s(X,Y, 19.8)	Qp	N/A	5,246	6.58

Table A8. Candidate DSMs for Dall's porpoises in the Salish Sea survey stratum, including response distributions (Qp=quasi-Poisson, Nb=negative binomial, Tw=Tweedie), deltaAIC values (within each response distribution), and dispersion statistics (values >1 indicate overdispersion and <1 indicate underdispersion). Non-linear smoother terms are enclosed in the notation 's( )' and the effective degrees of freedom of each term are also noted within the brackets. Models are listed in ascending order of deltaAIC within each response distribution and the selected best-fit model is highlighted in bold font. This candidate model set only includes one location-only s(X,Y) model (quasi-Poisson) because this covariate was not significant for Dall's porpoises in the Salish Sea for the other two error distributions tested. None of the negative binomial models that were tested contained any significant covariate terms, and so they are not shown here. The notation ~1 denotes a null model with no covariate terms.

Model covariates	Response distribution	deltaAIC	Estimated abundance	Dispersion statistic
s(dstShore, 0.9)	Tw	0	636	6.46
~ 1	Tw	1.5	505	9.06
s(dstShore, 1.6): Duchon spline	**Tw**	**2.2**	**580**	**6.22**
s(dstShore, 1.1)	Qp	N/A	656	5.29
s(X,Y, 12.9)	Qp	N/A	1168	2.03

Table A9. Candidate DSMs for harbour porpoises in the north coast survey stratum, including response distributions (Qp=quasi-Poisson, Nb=negative binomial, Tw=Tweedie), deltaAIC values (within each response distribution), and dispersion statistics (values >1 indicate overdispersion and <1 indicate underdispersion). Non-linear smoother terms are enclosed in the notation 's( )' and the effective degrees of freedom of each term are also noted within the brackets. Models are listed in ascending order of deltaAIC within each response distribution and the selected best-fit model is highlighted in bold font.

Model covariates	Response distribution	deltaAIC	Estimated abundance	Dispersion statistic
s(X,Y, 4.6) + s(depth, 2.7)	Nb	0	1,239	0.79
s(X,Y, 8.7)	**Nb**	**2.3**	**1,314**	**0.81**
s(X,Y, 10.2)	Tw	0	1,446	2.86
s(X,Y, 7.0) + s(depth, 2.4)	Tw	2.2	1,337	2.99
s(X,Y, 19.4)	Qp	N/A	1,301	1.26

Table A10. Candidate DSMs for harbour porpoises in the Salish Sea survey stratum, including response distributions (Qp=quasi-Poisson, Nb=negative binomial, Tw=Tweedie), deltaAIC values (within each response distribution), and dispersion statistics (values >1 indicate overdispersion and <1 indicate underdispersion). Non-linear smoother terms are enclosed in the notation 's( )' and the effective degrees of freedom of each term are also noted within the brackets. Models are listed in ascending order of deltaAIC within each response distribution and the selected best-fit model is highlighted in bold font.

Model covariates	Response distribution	deltaAIC	Estimated abundance	Dispersion statistic
s(X,Y, 20.1)	**Nb**	**0**	**3,893**	**0.62**
s(X,Y, 18.4) + s(depth, 0.9)	Nb	5.1	3,968	0.74
s(X,Y, 17.0) + s(depth, 1.0)	Tw	0	4,561	1.75
s(X,Y, 18.5)	Tw	2.2	4,203	1.58
s(X,Y, 21.6)	Qp	N/A	4,732	1.50

APPENDIX B. RELEVANT PACIFIC COAST GEOGRAPHIC NAMES

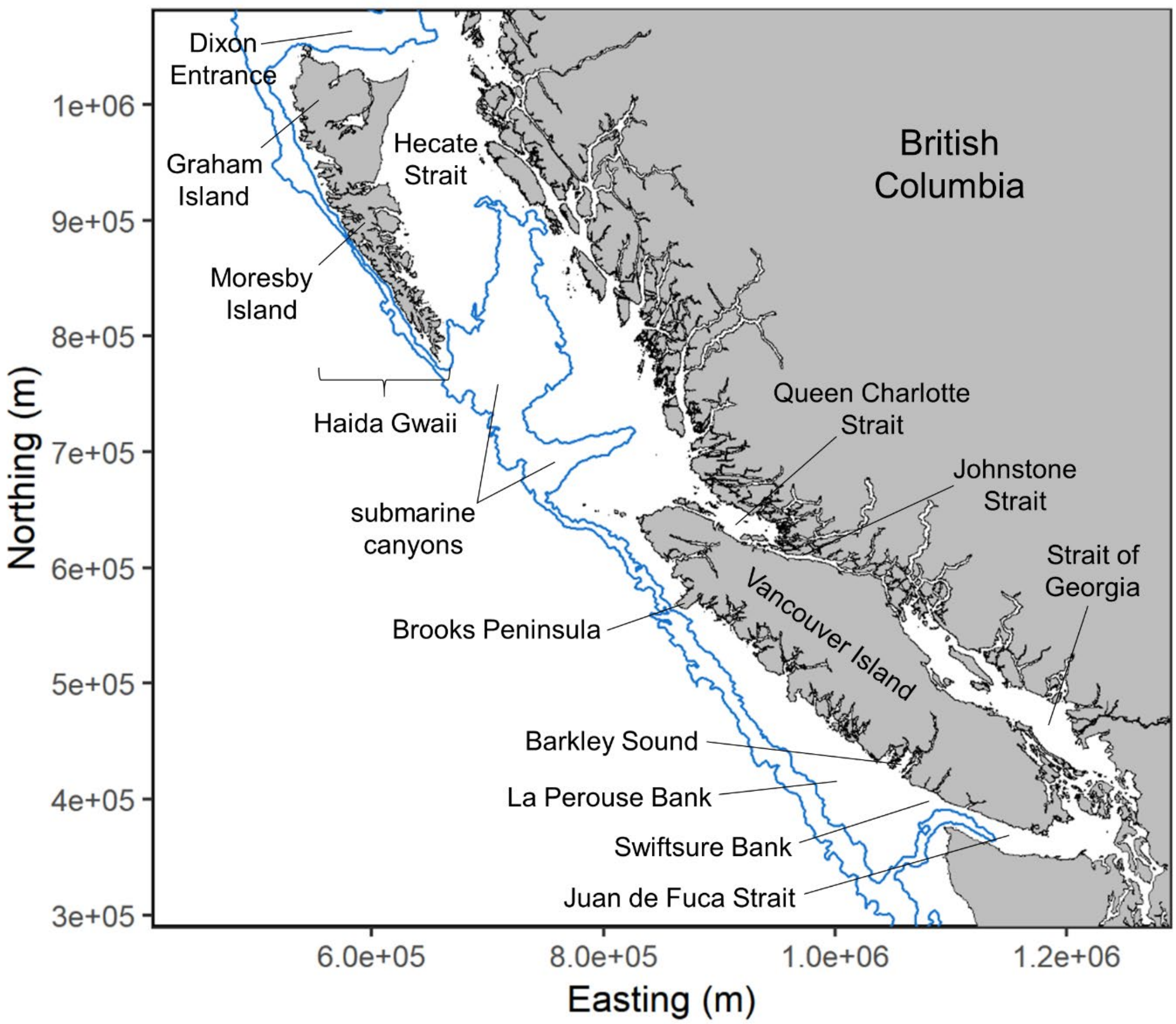

Figure B1. Map showing geographical names of the Canadian Pacific coast that are referred to in this report. Blue lines indicate the 200 and 1,000 m bathymetric contours.

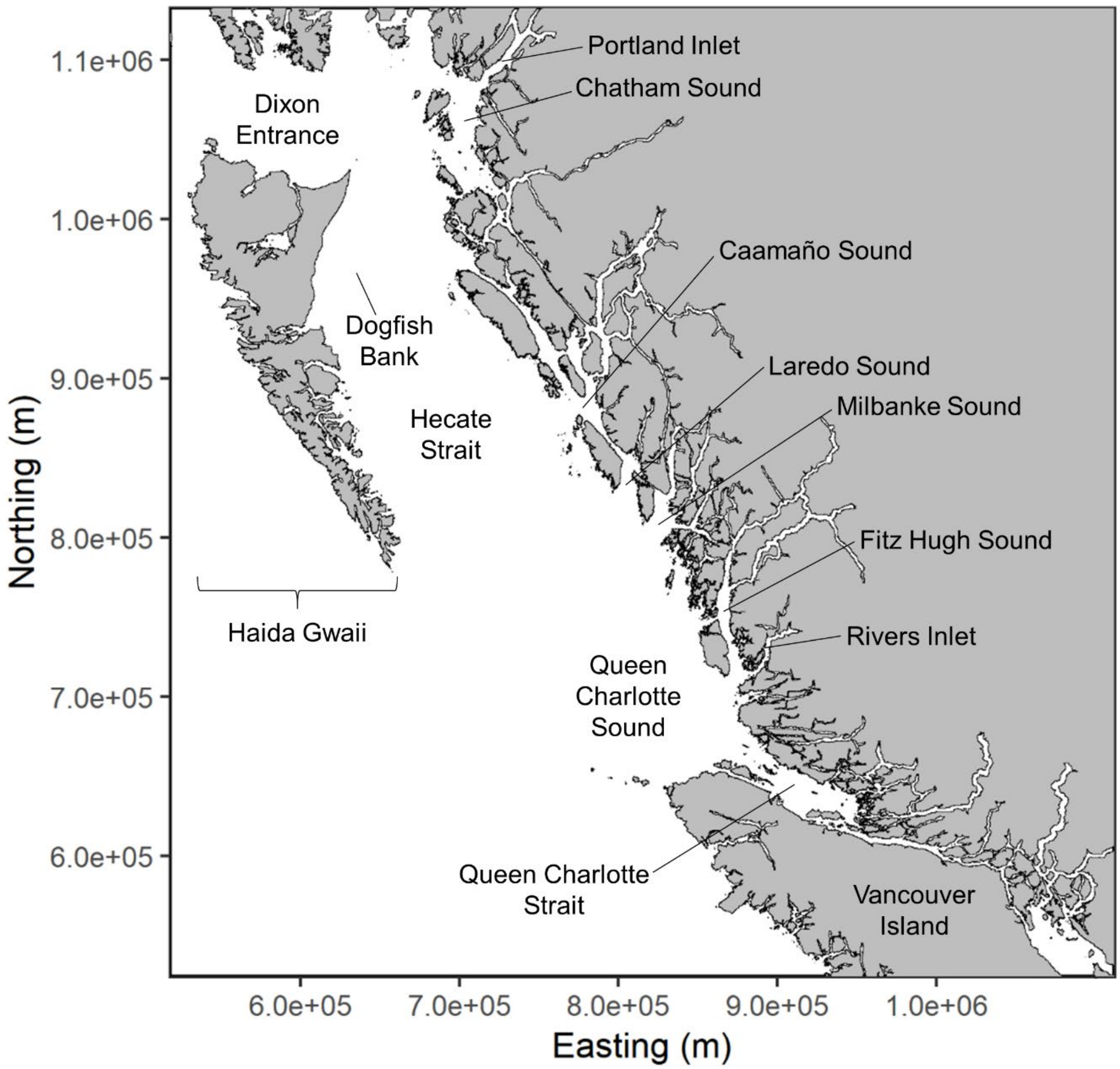

Figure B2. Map showing geographical names of the northern and central coasts of BC, Canada, that are referred to in this report.

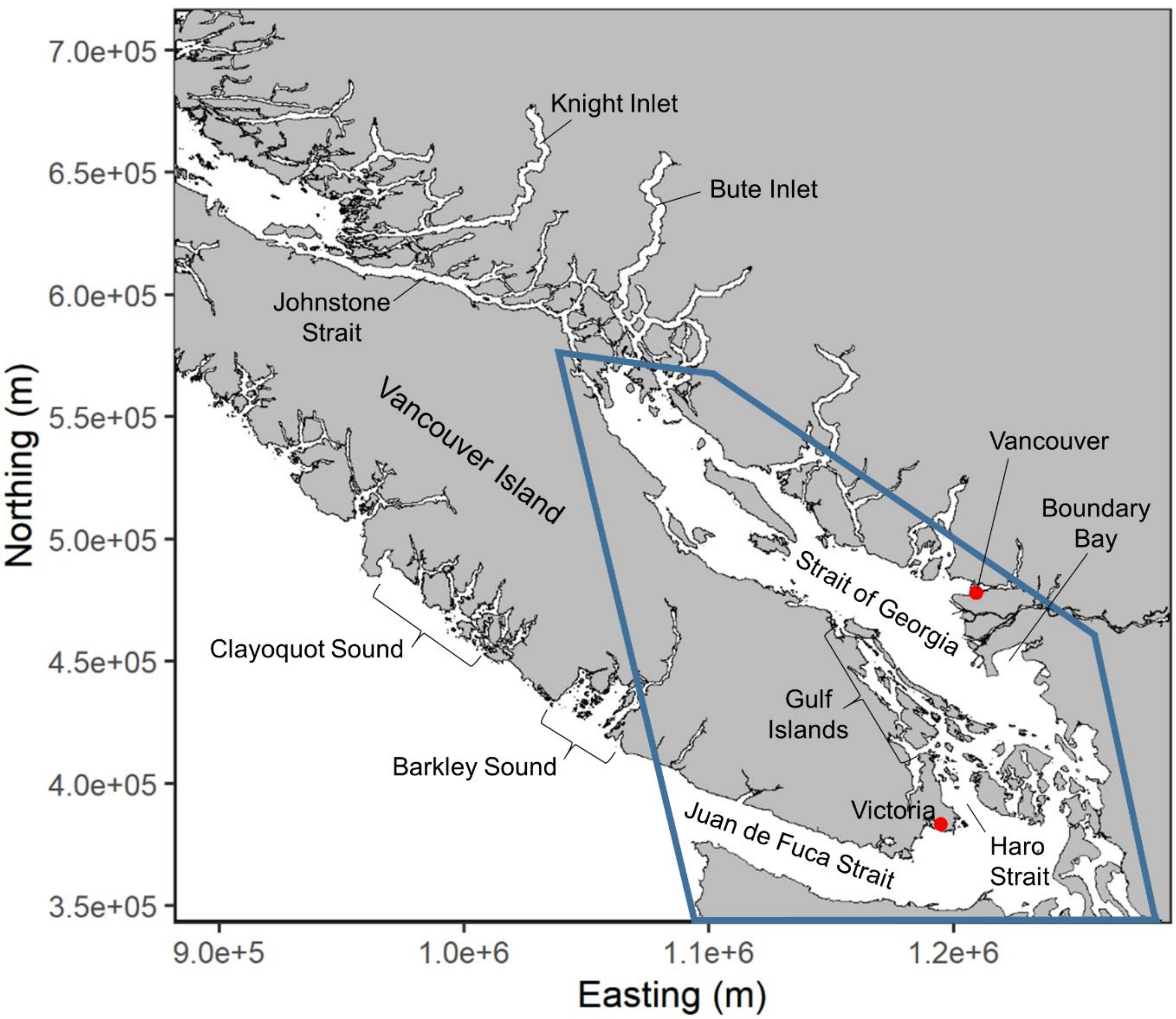

Figure B3. Map showing geographical names of the Salish Sea (area within the blue outline) and surrounding regions, BC, Canada, that are referred to in this report.